Appl. Numer. Math. 207 (2025) 174–192

Contents lists available at ScienceDirect

Applied Numerical Mathematics

journal homepage: www.elsevier.com/locate/apnum

Research Paper

An efficient uniformly convergent method for multi-scaled two dimensional parabolic singularly perturbed systems of convection-diffusion type

C. Clavero [a,b,*], J.C. Jorge [a,b]

[a] Department of Applied Mathematics and IUMA, University of Zaragoza, Spain
[b] Department of Computer Science, Mathematics and Statistics and ISC, Public University of Navarra, Pamplona, Spain

ARTICLE INFO

Keywords:
2D linear parabolic systems
Fractional implicit methods
Splitting
Shishkin meshes
Uniform convergence
Computational cost

ABSTRACT

In this work we solve initial-boundary value problems associated to coupled 2D parabolic singularly perturbed systems of convection-diffusion type. The analysis is focused on the cases where the diffusion parameters are small, distinct and also they may have different order of magnitude. In such cases, overlapping regular boundary layers appear at the outflow boundary of the spatial domain. The fully discrete scheme combines the classical upwind scheme defined on an appropriate Shishkin mesh to discretize the spatial variables, and the fractional implicit Euler method joins to a decomposition of the difference operator in directions and components to integrate in time. We prove that the resulting method is uniformly convergent of first order in time and of almost first order in space. Moreover, as only small tridiagonal linear systems must be solved to advance in time, the computational cost of our method is remarkably smaller than the corresponding ones to other implicit methods considered in the previous literature for the same type of problems. The numerical results, obtained for some test problems, corroborate in practice the good behavior and the advantages of the algorithm.

1. Introduction

Let us denote $\varepsilon = (\varepsilon_1, \varepsilon_2)^T$; in this paper, we develop a new technique to solve numerically in a robust and efficient way two dimensional parabolic singularly perturbed coupled convection-diffusion systems given by

$$\begin{cases} \mathcal{L}_\varepsilon(t)\mathbf{u} \equiv \dfrac{\partial \mathbf{u}}{\partial t}(\mathbf{x},t) + \mathcal{L}_{\mathbf{x},\varepsilon}(t)\mathbf{u}(\mathbf{x},t) = \mathbf{f}(\mathbf{x},t),\ (\mathbf{x},t) \in Q \equiv \Omega \times (0,T], \\ \mathbf{u}(\mathbf{x},t) = \mathbf{g}(\mathbf{x},t),\ (\mathbf{x},t) \in \partial\Omega \times [0,T], \\ \mathbf{u}(\mathbf{x},0) = \boldsymbol{\varphi}(\mathbf{x}),\ \mathbf{x} \in \Omega, \end{cases} \tag{1}$$

where $\Omega = (0,1)^2$, $\mathbf{x} = (x,y)^T$ and the spatial differential operator $\mathcal{L}_{\mathbf{x},\varepsilon}(t)$ is defined as

$$\mathcal{L}_{\mathbf{x},\varepsilon}(t)\mathbf{u} \equiv -\mathcal{D}_\varepsilon \Delta \mathbf{u} + \mathcal{B}_1(\mathbf{x})\frac{\partial \mathbf{u}}{\partial x}(\mathbf{x},t) + \mathcal{B}_2(\mathbf{x})\frac{\partial \mathbf{u}}{\partial y}(\mathbf{x},t) + \mathcal{A}(\mathbf{x},t)\mathbf{u}. \tag{2}$$

* Corresponding author.
E-mail addresses: clavero@unizar.es (C. Clavero), jcjorge@unavarra.es (J.C. Jorge).

https://doi.org/10.1016/j.apnum.2024.09.002
Received 8 March 2024; Received in revised form 5 July 2024; Accepted 3 September 2024

Available online 6 September 2024

The diffusion matrix is $D_\varepsilon = \mathrm{diag}(\varepsilon_1, \varepsilon_2)$ and we assume that the diffusion parameters ε_1 and ε_2 can be very small with $0 < \varepsilon_1 \leq \varepsilon_2 \leq 1$. The convection matrices are

$$\mathcal{B}_1(\mathbf{x}) = \mathrm{diag}(b_{11}(\mathbf{x}), b_{12}(\mathbf{x})), \quad \mathcal{B}_2(\mathbf{x}) = \mathrm{diag}(b_{21}(\mathbf{x}), b_{22}(\mathbf{x})),$$

where we assume that their diagonal coefficients $b_{rp}, r, p = 1, 2$ satisfy

$$b_{1r}(\mathbf{x}) \geq \beta_1 > 0, \ b_{2r}(\mathbf{x}) \geq \beta_2 > 0, \ r = 1, 2, \ \forall \ \mathbf{x} \in \overline{\Omega}, \tag{3}$$

for some positive constants β_1 and β_2. As well, we assume that $\forall (\mathbf{x}, t) \in \overline{Q}$ the coefficients of the reaction matrix $\mathcal{A}$ satisfy

$$a_{rr}(\mathbf{x}, t) \geq 0, \ a_{rp}(\mathbf{x}, t) \leq 0, \ \text{ if } \ r \neq p, \ r, p = 1, 2 \ \text{ and } \ \sum_{p=1}^{2} a_{rp}(\mathbf{x}, t) \geq 0, \ r = 1, 2. \tag{4}$$

Finally, we impose sufficient smoothness and compatibility conditions on $\mathbf{f}(\mathbf{x}, t) = (f_1, f_2)^T$, $\boldsymbol{\varphi}(\mathbf{x}) = (\varphi_1, \varphi_2)^T$, $\mathbf{g}(\mathbf{x}, t) = (g_1, g_2)^T$, $\mathcal{B}_1, \mathcal{B}_2, \mathcal{A}$ in order to get that the exact solution satisfies

$$\mathbf{u} \in C^{4,2}(\overline{Q}). \tag{5}$$

(see [27] for a detailed discussion)

Singularly perturbed systems take part in many mathematical models for different physical phenomena, such as saturated flows in fractured porous media, convective heat transport with large Péclet numbers, reaction-diffusion enzyme models, turbulent interactions of waves and currents, tubular models in chemical reactor theory, combustion processes, diffusion processes in electro-analytic chemistry or neutron transport models among many others (see for instance [2,17,21,35,37]). In the case of convection diffusion problems, for small values of the diffusion parameters, their solutions usually show a multiscale behavior, having boundary layers at the outflow boundary of Ω. Such behavior provokes that uniformly convergent methods are necessary to find a reliable and not too expensive numerical approximation; such methods are capable of providing a sufficiently precise numerical solution in the whole domain using meshes with a number of grid points which is independent of the size of the diffusion parameters.

In the past, many people have dealt with these problems for both reaction-diffusion and convection-diffusion systems. Linear elliptic or parabolic coupled systems were considered in [3,10,19,20,24,26,31,32,36] for one dimensional problems in space. In [34], a 1D elliptic convection-diffusion system, having distinct small diffusion coefficients at each equation, but also equal small parameters in the convective terms, was considered. In all of these works, uniformly convergent numerical schemes were constructed and analyzed. In the parabolic case, for the time integration processes, it is typical to resort to the backward Euler method, and the spatial discretization is done by using classical finite difference schemes, which are defined on special nonuniform meshes of Shishkin type. Using these tools, various uniformly convergent methods were constructed. Such methods have a common drawback coming from the calculus of the coupled components simultaneously; consequently, it is necessary to deal with large linear systems, with a band width which depends of the number of components in the system to integrate in time. A simple idea to reduce the computational cost in the time integration process consists of defining a method which decouples the calculus of the components in the system. Such idea was introduced in [7]; this technique, which the authors named splitting by components, separates the calculus of each component in such way that only tridiagonal systems must be solved to obtain the numerical solution, getting a remarkable reduction in the computational cost. Such reduction is more remarkable as long as higher dimensions in the system are considered. For the case of 2D elliptic or parabolic singularly perturbed systems of type (1), there are less references available. For instance, in [22,23] elliptic 2D singularly perturbed problems were considered and in [13] a 2D elliptic system of convection-diffusion type, having the same diffusion term in both equations and also equal small parameters in the convective terms, was studied. Another 2D elliptic system of convection-diffusion type was considered in [14]; in this case, distinct small parameters in the diffusion term and also equal small parameters in the convection terms were managed. In [8,16,25], various evolutionary 2D systems with two equations have been deeply studied and suitable numerical methods have been proposed to solve them successfully.

With respect to the drawbacks associated to the numerical solution of multidimensional problems, via finite differences, it is well known that the use of alternating direction implicit methods (see [33]) is an excellent choice to reduce the computational cost of the numerical algorithms, because only tridiagonal systems are involved in the integration in time. In [5], a method of this type was proposed for solving 2D scalar singularly perturbed diffusion-reaction problems and in [15] for the case of convection-diffusion problems. The same ideas can be applied for solving coupled systems, but the result it is not optimal in terms of their computational cost because, in these cases, still banded linear systems, are involved in the numerical integration in time. To elude this difficulty, we combine the ideas of [5,7] to construct a new numerical algorithm which combines the upwind scheme, defined on piecewise uniform Shishkin meshes, to discretize in space, and the fractional implicit Euler method, associated to a splitting both in directions and components, to integrate in time. In this way, simple small tridiagonal linear systems are required to solve at each time step and, consequently, a remarkable reduction in the computational cost is observed if we compare our proposal with any classical implicit method used for the same type of systems.

It is also well known that the use of one step methods to integrate in time initial-boundary value problems with non homogeneous boundary data, provokes additional difficulties, because it usually conduces to a reduction of the order of convergence for the derived numerical algorithms (see [1] and references therein). This phenomenon complicates the analysis of the uniform convergence when it appears. In our proposal, we have removed the possibility that this phenomenon produces in a simple way, based on a modified evaluation of the boundary data for some fractional steps.

The rest of the paper is structured as follows. In Section 2, we study the behavior of the exact solution of (1), proving appropriate estimates for its first partial derivatives in terms of the diffusion coefficients. In Section 3, we introduce the chosen spatial discretization and we prove its uniform convergence when it is defined on an special nonuniform mesh of Shishkin type. In Section 4, we describe the time integration process, via the fractional implicit Euler method joint to a splitting by directions and components and we prove that the fully discrete scheme is uniformly convergent of first order in time and of almost first order in space. In Section 5, the numerical results obtained with our algorithm for some test problems, are shown; from them, we corroborate in practice the theoretical results and the advantages of the proposed algorithm. We finish this work with a short section of conclusions.

In the rest of the paper, we denote $\|\cdot\|_D$ to the maximum norm for a function defined on the domain D, $\|\mathbf{w}\|_D = \max\{\|w_1\|_D, \|w_2\|_D\}$, $|\mathbf{v}| = (|v_1|, |v_2|)^T$, $\mathbf{v} \geq \mathbf{w}$ (analogously $\mathbf{v} \leq \mathbf{w}$) means $v_r \geq w_r, r = 1, 2$, and C is used to denote a generic positive constant which is independent of the diffusion and the discretization parameters ε, N and M; finally $\mathbf{C} \equiv (C, C)^T$.

2. Analytical properties of the exact solution

In this section we study the asymptotic behavior of the exact solution of problem (1) with respect to both diffusion parameters, obtaining sufficiently fine estimates for its first partial derivatives. These estimates will be used in the analysis of the uniform convergence for the numerical method proposed in this work.

With similar reasonings to the used ones in [13], we obtain the following two results, which give the inverse positivity and the uniform well posedness of the continuous problem.

Lemma 1. *(Maximum principle). Let $\mathcal{L}_\varepsilon(t)$ be the differential operator given in (1). If $\mathcal{L}_{\varepsilon r}(t)\boldsymbol{\Psi}(\mathbf{x},t) \geq \mathbf{0}, \boldsymbol{\Psi}(\mathbf{x},t) \geq \mathbf{0}, \ \forall (\mathbf{x},t) \in \partial\Omega \times [0,T]$ and $\boldsymbol{\Psi}(\mathbf{x},0) \geq \mathbf{0}, \ \forall \mathbf{x} \in \Omega$, then it holds $\boldsymbol{\Psi}(\mathbf{x},t) \geq \mathbf{0}, \ \forall (\mathbf{x},t) \in Q$.*

Lemma 2. *(Uniform well posedness). Let $\boldsymbol{\Psi}(\mathbf{x},t) \in C^{2,1}(Q)$; then, it holds*

$$\|\boldsymbol{\Psi}\| \leq \frac{1}{\beta}\|\mathcal{L}_\varepsilon(t)\boldsymbol{\Psi}\|_Q + \max\{\|\boldsymbol{\Psi}\|_{\partial\Omega\times[0,T]}, \|\boldsymbol{\Psi}(\mathbf{x},0)\|_{\mathbf{x}\in\Omega}\}$$

where

$$\beta = \min(\beta_1, \beta_2). \tag{6}$$

Following the ideas in [24], we can describe the time derivatives of $\mathbf{u}$ as solutions of initial-boundary value problems similar to (1) and again we can make use of Lemma 2 to prove that

$$\left|\frac{\partial^r \mathbf{u}(\mathbf{x},t)}{\partial t^r}\right| \leq C, \ r = 0, 1, 2, \tag{7}$$

i.e., the exact solution has uniformly bounded time derivatives up to order two.

Next, we search for appropriate estimates for the spatial derivatives of $\mathbf{u}$.

Lemma 3. *The solution $\mathbf{u}$ of (1) and its components $u_k, k = 1, 2$, satisfy*

$$\begin{aligned}
&\left|\frac{\partial^{(l_1+l_2)}\mathbf{u}(\mathbf{x},t)}{\partial x^{l_1}\partial y^{l_2}}\right| \leq C\boldsymbol{\varepsilon}^{-l_1-l_2}, \ 1 \leq l_1 + l_2 \leq 2,\\
&\left|\frac{\partial^{(l_1+l_2)}u_1(\mathbf{x},t)}{\partial x^{l_1}\partial y^{l_2}}\right| \leq C\varepsilon_1^{-l_1-l_2}, \ 3 \leq l_1 + l_2 \leq 4,\\
&\left|\frac{\partial^{(l_1+l_2)}u_2(\mathbf{x},t)}{\partial x^{l_1}\partial y^{l_2}}\right| \leq C\varepsilon_2^{-l_1-l_2} + C\varepsilon_1^{1-(l_1+l_2)/2}\varepsilon_2^{-1}, \ 3 \leq l_1 + l_2 \leq 4.
\end{aligned} \tag{8}$$

Proof. The proof uses the changes of variables $\Psi_1 = x/\varepsilon_1$, $\varphi_1 = y/\varepsilon_1$ for the first component and $\Psi_2 = x/\varepsilon_2$, $\varphi_2 = y/\varepsilon_2$ for the second component (see [13] for instance for more details). On the transformed problem, using the result in [27] we prove that, in the new variables, the derivatives are bounded independently of the singular perturbation parameters; therefore, in the original variables (x, y), the obtaining of the estimates (8) is immediate. □

Unfortunately, the bounds (8) are not fine enough to complete our later analysis because they do not describe the multi-scale behavior of $\mathbf{u}$. To get this, we decompose the exact solution as the sum of its regular component, named $\mathbf{v}$, its boundary layer component, $\mathbf{w}$ and its corner layer component, $\mathbf{p}_{rt}$. As well, we decompose the boundary layer component in two terms $\mathbf{w} = \mathbf{w}_r + \mathbf{w}_t$.

Let us denote the four sides of $\partial\Omega$ as

$$\Gamma_1 = \{(0,y) \,|\, 0 \leq y \leq 1\}, \quad \Gamma_2 = \{(x,0) \,|\, 0 \leq x \leq 1\},$$
$$\Gamma_3 = \{(1,y) \,|\, 0 \leq y \leq 1\}, \quad \Gamma_4 = \{(x,1) \,|\, 0 \leq x \leq 1\},$$

and let us denote by $\mathcal{L}_{\mathbf{x}}(t)$ the reduced first order hyperbolic differential operator given by

$$\mathcal{L}_{\mathbf{x}}(t)\mathbf{u} \equiv \frac{\partial \mathbf{u}}{\partial t}(\mathbf{x},t) + \mathcal{B}_1(\mathbf{x})\frac{\partial \mathbf{u}}{\partial x}(\mathbf{x},t) + \mathcal{B}_2(\mathbf{x})\frac{\partial \mathbf{u}}{\partial y}(\mathbf{x},t) + \mathcal{A}(\mathbf{x},t)\mathbf{u}. \tag{9}$$

These components are obtained as the solutions to the following problems:

$$\begin{cases} \mathcal{L}_{\mathbf{x},\varepsilon}(t)\mathbf{v}(\mathbf{x},t) = \mathbf{f}, & \forall (\mathbf{x},t) \in \Omega \times [0,T], \\ \mathbf{v}(\mathbf{x},t) = \psi_1(y,t), & \forall (\mathbf{x},t) \in \Gamma_1 \times [0,T], \\ \mathbf{v}(\mathbf{x},t) = \psi_2(x,t), & \forall (\mathbf{x},t) \in \Gamma_2 \times [0,T], \\ \mathbf{v}(\mathbf{x},t) = \psi_3(y,t), & \forall (\mathbf{x},t) \in \Gamma_3 \times [0,T], \\ \mathbf{v}(\mathbf{x},t) = \psi_4(x,t), & \forall (\mathbf{x},t) \in \Gamma_4 \times [0,T], \\ \mathbf{v}(\mathbf{x},0) = \boldsymbol{\varphi}(\mathbf{x}), & \mathbf{x} \in \Omega, \end{cases} \tag{10}$$

where $\psi_i,\ i = 1,2,3,4$ are appropriate functions which will be stated in the posterior analysis,

$$\begin{cases} \mathcal{L}_{\mathbf{x},\varepsilon}(t)\mathbf{w}_k(\mathbf{x},t) = \mathbf{0},\ k = r,t, & \forall (\mathbf{x},t) \in \Omega \times [0,T], \\ \mathbf{w}_r(\mathbf{x},t) = (\mathbf{u}-\mathbf{v})(\mathbf{x},t), & \forall (\mathbf{x},t) \in \Gamma_3 \times [0,T], \\ \mathbf{w}_r(\mathbf{x},t) = 0, & \forall (\mathbf{x},t) \in \Gamma_1 \cup \Gamma_2 \cup \Gamma_4 \times [0,T], \\ \mathbf{w}_t(\mathbf{x},t) = (\mathbf{u}-\mathbf{v})(\mathbf{x},t), & \forall (\mathbf{x},t) \in \Gamma_4 \times [0,T], \\ \mathbf{w}_t(\mathbf{x},t) = 0, & \forall (\mathbf{x},t) \in \Gamma_1 \cup \Gamma_2 \cup \Gamma_3 \times [0,T], \\ \mathbf{w}_k(\mathbf{x},0) = \mathbf{0}, & \mathbf{x} \in \Omega, \end{cases} \tag{11}$$

for the boundary layer components, and

$$\begin{cases} \mathcal{L}_{\mathbf{x},\varepsilon}(t)\mathbf{p}_{rt}(\mathbf{x},t) = \mathbf{0}, & \forall (\mathbf{x},t) \in \Omega \times [0,T], \\ \mathbf{p}_{rt}(\mathbf{x},t) = -\mathbf{w}_r(\mathbf{x},t), & \forall (\mathbf{x},t), \in \Gamma_3 \times [0,T], \\ \mathbf{p}_{rt}(\mathbf{x},t) = -\mathbf{w}_t(\mathbf{x},t), & \forall (\mathbf{x},t), \in \Gamma_4 \times [0,T], \\ \mathbf{p}_{rt}(\mathbf{x},t) = 0, & \forall (\mathbf{x},t), \in \Gamma_1 \cup \Gamma_2 \times [0,T], \\ \mathbf{p}_{rt}(\mathbf{x},0) = \mathbf{0}, & \mathbf{x} \in \Omega, \end{cases} \tag{12}$$

for the corner layer component, respectively.

Lemma 4. *Let $\boldsymbol{v} = (v_1, v_2)^T$ be the regular component solution of (10). Then, its derivatives satisfy*

$$\begin{aligned} &\left\| \frac{\partial^{l_1+l_2}\boldsymbol{v}(\mathbf{x},t)}{\partial x^{l_1}\partial y^{l_2}} \right\| \le C,\ 0 \le l_1 + l_2 \le 2, \left\| \frac{\partial^{l_1+l_2} v_1(\mathbf{x},t)}{\partial x^{l_1}\partial y^{l_2}} \right\| \le C\varepsilon_1^{-1},\ l_1 + l_2 = 3, \\ &\left\| \frac{\partial^{l_1+l_2} v_2(\mathbf{x},t)}{\partial x^{l_1}\partial y^{l_2}} \right\| \le C,\ l_1 + l_2 = 3. \end{aligned} \tag{13}$$

Proof. The proof follows similar ideas and techniques that those ones in [14], where full details of the proof for an elliptic system can be seen.

In the first step, the regular component is decomposed as

$$\mathbf{v} = \chi_0 + \varepsilon_2\chi_1 + \varepsilon_2^2\chi_2 + \varepsilon_2^3\chi_3, \tag{14}$$

where $\chi_i = (\chi_{i1}, \chi_{i2})^T$, $i = 0,1,2,3$, and their respective equations on $\overline{Q}$ are the followings:

$$\begin{aligned} &\mathcal{L}_{\mathbf{x}}(t)\chi_0 = \mathbf{f},\ \chi_0(\mathbf{x},t) = \mathbf{u}(\mathbf{x},t),\ \forall (\mathbf{x},t) \in \Gamma_1 \cup \Gamma_2 \times [0,T],\ \chi_0(\mathbf{x},0) = \varphi(\mathbf{x}), \mathbf{x} \in \Omega, \\ &\mathcal{L}_{\mathbf{x}}(t)\chi_1 = \frac{1}{\varepsilon_2}D_\varepsilon\Delta\chi_0,\ \chi_1(\mathbf{x},t) = \mathbf{0},\ \forall (\mathbf{x},t) \in \Gamma_1 \cup \Gamma_2 \times [0,T],\ \chi_1(\mathbf{x},0) = \mathbf{0}, \mathbf{x} \in \Omega, \\ &\mathcal{L}_{\mathbf{x}}(t)\chi_2 = \frac{1}{\varepsilon_2}D_\varepsilon\Delta\chi_1,\ \chi_2(\mathbf{x},t) = \mathbf{0},\ \forall (\mathbf{x},t) \in \Gamma_1 \cup \Gamma_2 \times [0,T],\ \chi_2(\mathbf{x},0) = \mathbf{0}, \mathbf{x} \in \Omega, \\ &\mathcal{L}_{\mathbf{x},\varepsilon}(t)\chi_3 = \frac{1}{\varepsilon_2}D_\varepsilon\Delta\chi_2,\ \chi_3(\mathbf{x},t) = \mathbf{0},\ \forall (\mathbf{x},t) \in \partial\Omega \times [0,T],\ \chi_3(\mathbf{x},0) = \mathbf{0}, \mathbf{x} \in \Omega. \end{aligned} \tag{15}$$

From (14), it is straightforward that it holds

$$\left\| \frac{\partial^{l_1+l_2}\chi_i}{\partial x^{l_1}\partial y^{l_2}} \right\| \le C,\ 0 \le i \le 2,\ 0 \le l_1 + l_2 \le 3.$$

To find bounds for the derivatives of the components of χ_3, for its second component, using Lemma 3 it follows (see [14] for more details)

$$\left\| \frac{\partial^{l_1+l_2}\chi_{32}}{\partial x^{l_1}\partial y^{l_2}} \right\| \leq C\varepsilon_2^{-l_1-l_2},\ 0 \leq l_1+l_2 \leq 3.$$

Also, using the equation in (15) which defines χ_{31}, we deduce estimates for χ_{31} and its derivatives; to do that, we split χ_{31} in the form

$$\chi_{31} = \psi_0 + \varepsilon_1\psi_1 + \varepsilon_1^2\psi_2 + \varepsilon_1^3\psi_3,$$

where the equations for ψ_i, $i = 0,1,2,3$ are given by

$$(\psi_0)_t + (b_{11}, b_{21})\cdot\nabla\psi_0 + a_{11}\psi_0 = -\frac{\varepsilon_1}{\varepsilon_2}\Delta\chi_{21} - a_{12}\chi_{32}, \tag{16a}$$

$$\psi_0(\mathbf{x},t) = 0,\ \forall(\mathbf{x},t)\in\Gamma_1\cup\Gamma_2\times[0,T],\ \psi_0(\mathbf{x},0) = \mathbf{0}, \mathbf{x}\in\Omega,$$

$$(\psi_1)_t + (b_{11}, b_{21})\cdot\nabla\psi_1 + a_{11}\psi_1 = \Delta\psi_0, \tag{16b}$$

$$\psi_1(\mathbf{x},t) = 0,\ \forall(\mathbf{x},t)\in\Gamma_1\cup\Gamma_2\times[0,T],\ \psi_1(\mathbf{x},0) = \mathbf{0}, \mathbf{x}\in\Omega,$$

$$(\psi_2)_t + (b_{11}, b_{21})\cdot\nabla\psi_2 + a_{11}\psi_2 = \Delta\psi_1, \tag{16c}$$

$$\psi_2(\mathbf{x},t) = 0,\ \forall(\mathbf{x},t)\in\Gamma_1\cup\Gamma_2\times[0,T],\ \psi_2(\mathbf{x},0) = \mathbf{0}, \mathbf{x}\in\Omega,$$

$$(\psi_0)_t - \varepsilon_1\Delta\psi_3 + (b_{11}, b_{21})\cdot\nabla\psi_3 + a_{11}\psi_3 = \Delta\psi_2, \tag{16d}$$

$$\psi_3(\mathbf{x},t) = 0,\ \forall(\mathbf{x},t)\in\partial\Omega\times[0,T],\ \psi_3(\mathbf{x},0) = \mathbf{0}, \mathbf{x}\in\Omega.$$

Then, from (16a)-(16c), it can be proved the following estimates:

$$\left\| \frac{\partial^{l_1+l_2}\psi_0}{\partial x^{l_1}\partial y^{l_2}} \right\| \leq C\varepsilon_2^{1-l_1-l_2},\ 0 \leq l_1+l_2 \leq 3,$$

$$\left\| \frac{\partial^{l_1+l_2}\psi_1}{\partial x^{l_1}\partial y^{l_2}} \right\| \leq C\varepsilon_2^{-l_1-l_2},\ 0 \leq l_1+l_2 \leq 3,$$

$$\left\| \frac{\partial^{l_1+l_2}\psi_2}{\partial x^{l_1}\partial y^{l_2}} \right\| \leq C\varepsilon_2^{-2},\ 0 \leq l_1+l_2 \leq 1,$$

$$\left\| \frac{\partial^{l_1+l_2}\psi_2}{\partial x^{l_1}\partial y^{l_2}} \right\| \leq C\varepsilon_2^{-1-l_1-l_2} + C\varepsilon_1^{1-l_1-l_2}\varepsilon_2^{-1},\ 2 \leq l_1+l_2 \leq 3.$$

Moreover, we can obtain

$$\left\| \frac{\partial^{l_1+l_2}\psi_3}{\partial x^{l_1}\partial y^{l_2}} \right\| \leq C\varepsilon_1^{-l_1-l_2}\varepsilon_2^{-3} + C\varepsilon_1^{1-l_1-l_2}\varepsilon_2^{-1},\ 0 \leq l_1+l_2 \leq 3.$$

Now, writing

$$\chi_{31}(\mathbf{x},t) = \psi_0 + \varepsilon_1\psi_1 + \varepsilon_1^2\psi_2,\ \forall(\mathbf{x},t)\in\Gamma_1\cup\Gamma_2\times[0,T], \tag{17}$$

we deduce that it holds

$$\left\| \frac{\partial^{l_1+l_2}\chi_{31}}{\partial x^{l_1}\partial y^{l_2}} \right\| \leq C,\ 0 \leq l_1+l_2 = 1,\ \left\| \frac{\partial^{l_1+l_2}\chi_{31}}{\partial x^{l_1}\partial y^{l_2}} \right\| \leq C\varepsilon_2^{-1},\ l_1+l_2 = 2,$$

$$\left\| \frac{\partial^{l_1+l_2}\chi_{31}}{\partial x^{l_1}\partial y^{l_2}} \right\| \leq C\varepsilon_1^{-1} + C\varepsilon_2^{-2},\ l_1+l_2 = 3.$$

Applying the bounds on χ_{31} and its derivatives to the equation of χ_{32}, the second component of χ_3 in (15), we have

$$\left\| \frac{\partial^{l_1+l_2}\chi_{32}}{\partial x^{l_1}\partial y^{l_2}} \right\| \leq C\varepsilon_2^{-3},\ l_1+l_2 = 3.$$

From all the above bounds, the required result follows. □

In second place, we study the asymptotic behavior of the layer components $\mathbf{w}_r$ and $\mathbf{w}_t$. To simplify the notation, we introduce the layer functions $\mathcal{B}_i(x)$ and $\mathcal{B}_i(y)$, $i = 1,2$, which are given by

$$\begin{array}{ll} \mathcal{B}_1(x) = e^{-\beta(1-x)/\varepsilon_1}, & \mathcal{B}_2(x) = e^{-\beta(1-x)/\varepsilon_2}, \\ \mathcal{B}_1(y) = e^{-\beta(1-y)/\varepsilon_1}, & \mathcal{B}_2(y) = e^{-\beta(1-y)/\varepsilon_2}, \end{array} \tag{18}$$

where β is defined in (6).

Lemma 5. *Let $\boldsymbol{w}_k$, $k = r, t$, where $\boldsymbol{w}_k = (w_{k1}, w_{k2})^T$ satisfy the problem (11). Then, the following bounds hold for the singular components:*

$$
\begin{aligned}
&|w_{r1}(\mathbf{x},t)| \le C\mathcal{B}_2(x),\ |w_{r2}(\mathbf{x},t)| \le C\mathcal{B}_2(x),\\
&|w_{t1}(\mathbf{x},t)| \le C\mathcal{B}_2(y),\ |w_{t2}(\mathbf{x},t)| \le C\mathcal{B}_2(y),\\
&\left|\frac{\partial^{i+j} w_{r1}(\mathbf{x},t)}{\partial x^i \partial y^j}\right| \le C(\varepsilon_1^{-i}\mathcal{B}_1(x) + \varepsilon_2^{-i}\mathcal{B}_2(x)),\ i,j = 1,2,3,\\
&\left|\frac{\partial^{i+j} w_{t1}(\mathbf{x},t)}{\partial x^i \partial y^j}\right| \le C(\varepsilon_1^{-j}\mathcal{B}_1(y) + \varepsilon_2^{-j}\mathcal{B}_2(y)),\ i,j = 1,2,3,\\
&\left|\frac{\partial^{i+j} w_{r2}(\mathbf{x},t)}{\partial x^i \partial y^j}\right| \le C\varepsilon_2^{-i}\mathcal{B}_2(x),\ i,j = 1,2,\\
&\left|\frac{\partial^{i+j} w_{r2}(\mathbf{x},t)}{\partial x^i \partial y^j}\right| \le C\left(\varepsilon_1^{-1}\varepsilon_2^{-2}\mathcal{B}_1(x) + \varepsilon_2^{-3}\mathcal{B}_2(x)\right),\ i,j = 3,\\
&\left|\frac{\partial^{i+j} w_{t2}(\mathbf{x},t)}{\partial x^i \partial y^j}\right| \le C\varepsilon_2^{-j}\mathcal{B}_2(y),\ i,j = 1,2,\\
&\left|\frac{\partial^{i+j} w_{t2}(\mathbf{x},t)}{\partial x^i \partial y^j}\right| \le C\left(\varepsilon_1^{-1}\varepsilon_2^{-2}\mathcal{B}_1(y) + \varepsilon_2^{-3}\mathcal{B}_2(y)\right),\ i,j = 3.
\end{aligned}
$$

Proof. To prove the estimates for the derivatives of the layer components, we again use the idea of change of variables. Here, we only show the details to obtain the bounds for the right layer component $\mathbf{w}_r$, and similarly we can proceed for $\mathbf{w}_t$.

We consider the change of variable $\Psi_1 = x/\nu_1$, $\Psi_2 = x/\nu_2$, where

$$
\nu_1 = \varepsilon_1(1+\sqrt{\varepsilon_1})^{-1},\ \nu_2 = \varepsilon_2(1+\sqrt{\varepsilon_2})^{-1}. \tag{19}
$$

Then, the resulting problems obtained after these changes of variables are given by

$$
\begin{aligned}
&\frac{\partial w^*_{r1}}{\partial t} - \left(\varepsilon_1\nu_1^{-2}\frac{\partial^2 w^*_{r1}}{\partial \Psi_1^2} + \varepsilon_1\frac{\partial^2 w^*_{r1}}{\partial y^2}\right) + \nu_1^{-1}b^*_{11}(\Psi_1,y)\frac{\partial w^*_{r1}}{\partial \Psi_1} + b^*_{21}(\Psi_1,y)\frac{\partial w^*_{r1}}{\partial y} +\\
&a^*_{11}(\Psi_1,y,t)w^*_{r1} + a^*_{12}(\Psi_1,y,t)w^*_{r2} = 0, \quad \forall(\Psi_1,y,t) \in \Omega^{*,1}_{\nu_1}\times[0,T],\\
&w^*_{r1}(\Psi_1,y,t) = (u^*_1 - v^*_1)(\Psi_1,y,t), \quad \forall(\Psi_1,y,t) \in \Gamma^{*,1}_{3,\nu_1}\times[0,T],\\
&w^*_{r1}(\Psi_1,y,t) = 0, \quad \forall(\Psi_1,y,t) \in \Gamma^{*,1}_{1,\nu_1}\cup\Gamma^{*,1}_{2,\nu_1}\cup\Gamma^{*,1}_{3,\nu_1}\times[0,T],\\
&w^*_{r1}(\Psi_1,y,0) = 0, \quad \forall(\Psi_1,y) \in \Omega^{*,1}_{\nu_1},
\end{aligned}
$$

and

$$
\begin{aligned}
&\frac{\partial w^*_{r2}}{\partial t} - \left(\varepsilon_2\nu_2^{-2}\frac{\partial^2 w^*_{r2}}{\partial \Psi_2^2} + \varepsilon_2\frac{\partial^2 w^*_{r2}}{\partial y^2}\right) + \nu_2^{-1}b^*_{12}(\Psi_2,y)\frac{\partial w^*_{r2}}{\partial \Psi_2} + b^*_{22}(\Psi_2,y)\frac{\partial w^*_{r2}}{\partial y} +\\
&a^*_{21}(\Psi_2,y,t)w^*_{r2} + a^*_{22}(\Psi_2,y,t)w^*_{r2} = 0, \quad \forall(\Psi_2,y,t) \in \Omega^{*,1}_{\nu_2}\times[0,T],\\
&w^*_{r2}(\Psi_2,y,t) = (u^*_2 - v^*_2)(\Psi_2,y,t), \quad \forall(\Psi_2,y,t) \in \Gamma^{*,1}_{3,\nu_1}\times[0,T],\\
&w^*_{r2}(\Psi_2,y,t) = 0, \quad \forall(\Psi_2,y,t) \in \Gamma^{*,1}_{1,\nu_1}\cup\Gamma^{*,1}_{2,\nu_1}\cup\Gamma^{*,1}_{3,\nu_1}\times[0,T],\\
&w^*_{r2}(\Psi_2,y,0) = 0, \quad \forall(\Psi_2,y) \in \Omega^{*,1}_{\nu_2},
\end{aligned}
$$

respectively, where $\Omega^{*,1}_{\nu_1} = (0,1/\nu_1)\times(0,1)$, $\Omega^{*,1}_{\nu_2} = (0,1/\nu_2)\times(0,1)$ and $\Gamma^{*,1}_{i,\nu_1}$, $\Gamma^{*,1}_{i,\nu_2}$, $i = 1,2,3,4$ are the corresponding boundaries of the extended domain $\Omega^{*,1}_{\nu_1}$ and $\Omega^{*,1}_{\nu_2}$, respectively.

Following a similar technique that this one in [4,29], we can obtain appropriate estimates for the right layer component $\mathbf{w}^*_r$. Therefore, in the original variables, the required result follows. □

To finish the study of the asymptotic behavior of the exact solution of the continuous problem, we study the estimates for the derivatives of the corner layer component $\mathbf{p}_{rt}$.

Lemma 6. *Let $\boldsymbol{p}_{rt}$, where $\boldsymbol{p}_{rt} = (p_{rt_1}, p_{rt_2})^T$, be the solution of the problem (12). Then, it holds*

$$
\begin{aligned}
&|\boldsymbol{p}_{rt}(\mathbf{x},t)| \le C\mathcal{B}_2(x)\mathcal{B}_2(y),\\
&\left|\frac{\partial^{i+j} p_{rt_1}(\mathbf{x},t)}{\partial x^i \partial y^j}\right| \le C\left(\varepsilon_1^{-i-j}\mathcal{B}_1(x)\mathcal{B}_1(y) + \varepsilon_2^{-i-j}\mathcal{B}_2(x)\mathcal{B}_2(y)\right),\ 1 \le i+j \le 3,\\
&\left|\frac{\partial^{i+j} p_{rt_2}(\mathbf{x},t)}{\partial x^i \partial y^j}\right| \le C\varepsilon_2^{-i-j}\mathcal{B}_2(x)\mathcal{B}_2(y),\ 1 \le i+j \le 2,
\end{aligned}
$$

Proof. Again, we use the idea of change of variables. Now, we take $\Psi_1 = x/\nu_1$, $\varphi_1 = y/\nu_1$, and $\Psi_2 = x/\nu_2$, $\varphi_2 = y/\nu_2$, where ν_1 and ν_2 are given in (19). Then, the resulting continuous problems obtained after these changes of variables are given by

$$\begin{aligned}
&\frac{\partial p^*_{rt_1}}{\partial t} - \varepsilon_1 \nu_1^{-2}\left(\frac{\partial^2 p^*_{rt_1}}{\partial \Psi_1^2} + \frac{\partial^2 p^*_{rt_1}}{\partial \varphi_1^2}\right) + \nu_1^{-1}\left(b^*_{11}(\Psi_1,\varphi_1)\frac{\partial p^*_{rt_1}}{\partial \Psi_1} + b^*_{21}(\Psi_1,\varphi_1)\frac{\partial p^*_{rt_1}}{\partial \varphi_1}\right) + \\
&a^*_{11}(\Psi_1,\varphi_1,t)p^*_{rt_1} + a^*_{12}(\Psi_1,\varphi_1,t)p^*_{rt_2} = 0,\ \forall (\Psi_1,\varphi_1,t) \in \Omega^{*,2}_{\nu_1} \times [0,T], \\
&p^*_{rt_1}(\Psi_1,\varphi_1,t) = -w^*_{r1}(\Psi_1,\varphi_1,t), \quad \forall (\Psi_1,\varphi_1,t) \in \Gamma^{*,2}_{3,\nu_1} \times [0,T], \\
&p^*_{rt_1}(\Psi_1,\varphi_1,t) = -w^*_{t1}(\Psi_1,\varphi_1,t), \quad \forall (\Psi_1,\varphi_1,t) \in \Gamma^{*,2}_{4,\nu_1} \times [0,T], \\
&p^*_{rt_1}(\Psi_1,\varphi_1,t) = 0,\ \forall (\Psi_1,\varphi_1,t) \in \Gamma^{*,2}_{1,\nu_1} \cup \Gamma^{*,2}_{1,\nu_1} \times [0,T], \\
&p^*_{rt_1}(\Psi_1,\varphi_1,0) = 0, \forall (\Psi_1,\varphi_1) \in \Omega^{*,2}_{\nu_1},
\end{aligned}$$

and

$$\begin{aligned}
&\frac{\partial p^*_{rt_2}}{\partial t} - \varepsilon_2 \nu_2^{-2}\left(\frac{\partial^2 p^*_{rt_2}}{\partial \Psi_2^2} + \frac{\partial^2 p^*_{rt_2}}{\partial \varphi_2^2}\right) + \nu_2^{-1}\left(b^*_{12}(\Psi_2,\varphi_2)\frac{\partial p^*_{rt_2}}{\partial \Psi_2} + b^*_{22}(\Psi_2,\varphi_2)\frac{\partial p^*_{rt_2}}{\partial \varphi_2}\right) + \\
&a^*_{21}(\Psi_2,\varphi_2,t)p^*_{rt_2} + a^*_{22}(\Psi_2,\varphi_2,t)p^*_{rt_2} = 0,\ \forall (\Psi_2,\varphi_2,t) \in \Omega^{*,2}_{\nu_2} \times [0,T], \\
&p^*_{rt_2}(\Psi_2,\varphi_2,t) = -w^*_{r2}(\Psi_2,\varphi_2,t), \quad \forall (\Psi_2,\varphi_2,t) \in \Gamma^{*,2}_{3,\nu_2} \times [0,T], \\
&p^*_{rt_2}(\Psi_2,\varphi_2,t) = -w^*_{t2}(\Psi_2,\varphi_2,t), \quad \forall (\Psi_2,\varphi_2,t) \in \Gamma^{*,2}_{4,\nu_2} \times [0,T], \\
&p^*_{rt_2}(\Psi_2,\varphi_2,t) = 0,\ \forall (\Psi_2,\varphi_2,t) \in \Gamma^{*,2}_{1,\nu_2} \cup \Gamma^{*,2}_{1,\nu_2} \times [0,T], \\
&p^*_{rt_2}(\Psi_2,\varphi_2,0) = 0, \forall (\Psi_2,\varphi_2) \in \Omega^{*,2}_{\nu_2},
\end{aligned}$$

respectively, where $\Omega^{*,1}_{\nu_1} = (0, 1/\nu_1) \times (0,1)$, $\Omega^{*,1}_{\nu_2} = (0, 1/\nu_2) \times (0,1)$ and $\Gamma^{*,2}_{i,\nu_1}$, $\Gamma^{*,2}_{i,\nu_2}$, $i = 1,2,3,4$ are the corresponding boundaries of the extended domain $\Omega^{*,2}_{\nu_1}$ and $\Omega^{*,2}_{\nu_2}$, respectively.

Using a similar methodology that in [4,28], we can get the bounds for the corner layer component $\mathbf{p}^*_{rt}$. Therefore, in the original variables, the required result follows. □

3. The spatial discretization

In this section we construct the spatial mesh and we define the spatial discretization of the continuous problem (1) and we prove its uniform convergence, showing that the semidiscrete scheme, obtained with our discretization, converges uniformly to the exact solution with almost first order.

The first step to discretize in space the continuous problem (1) consists of constructing a rectangular mesh, which is the tensor product of one dimensional piecewise uniform meshes of Shishkin type, i.e., $\overline{\Omega}^N = \overline{I}^N_x \times \overline{I}^N_y$, with $\overline{I}^N_x = \{0 = x_0 < x_1 < \ldots, < x_N = 1\}$, $\overline{I}^N_y = \{0 = y_0 < y_1 < \ldots, < y_N = 1\}$. For simplicity in the analysis, we have taken the same number of grid points, $N+1$, for both spatial directions.

From the previous section, we know that the exact solution has overlapping regular boundary layers of widths $\mathcal{O}(\varepsilon_1)$ and $\mathcal{O}(\varepsilon_2)$, respectively, which appear on the outflow domain of Ω. Then, we define $\overline{I}^N_x$ (and similarly we can proceed for $\overline{I}^N_y$) as follows (see [30]). Let N be multiple of 3; then, the grid points of $\bar{I}^N_x$ are given by

$$x_i = \begin{cases} iH, & i = 0, \ldots, N/3, \\ x_{N/3} + (i - N/3)h_1, & i = N/3+1, \ldots, 2N/3, \\ x_{2N/3} + (i - 2N/3)h_2, & i = 2N/3+1, \ldots, N, \end{cases} \tag{20}$$

where $H = 3(1-\sigma_2)/N$, $h_1 = 3(\sigma_2 - \sigma_1)/N$, $h_2 = 3\sigma_1/N$, and the transition parameters σ_1, σ_2 are defined by

$$\sigma_2 = \min\left\{2/3, \sigma_0 \varepsilon_2 \ln N\right\}, \quad \sigma_1 = \min\left\{\sigma_2/2, \sigma_0 \varepsilon_1 \ln N\right\}, \tag{21}$$

being σ_0 a constant which will be precise later on. We denote $h_{x,i} = x_i - x_{i-1}$, $h_{y,j} = y_j - y_{j-1}$, $i,j = 1, \ldots, N$, $\overline{h}_{x,i} = (h_{x,i} + h_{x,i+1})/2$ and $\overline{h}_{y,j} = (h_{y,j} + h_{y,j+1})/2$, $i,j = 1, \ldots, N-1$.

Following to the notation used for the continuous problem, the boundaries of the domain $\overline{\Omega}^N$ are denoted by

$$\Gamma^N_1 = \left\{(0, y_j) \,\middle|\, 0 \le j \le N\right\}, \Gamma^N_2 = \left\{(x_i, 0) \,\middle|\, 0 \le i \le N\right\},$$

$$\Gamma^N_3 = \left\{(1, y_j) \,\middle|\, 0 \le j \le N\right\}, \Gamma^N_4 = \left\{(x_i, 1) \,\middle|\, 0 \le i \le N\right\},$$

and $\partial\Omega^N = \Gamma^N_1 \cup \Gamma^N_2 \cup \Gamma^N_3 \cup \Gamma^N_4$.

Let us denote by Ω^N the subgrid of $\overline{\Omega}^N$ composed only by the interior points of it, i.e., by $\overline{\Omega}^N \bigcap \Omega$, $\partial\Omega^N \equiv \overline{\Omega}^N \backslash \Omega^N$, by $[\mathbf{v}]_{\Omega^N}$ (analogously $[v]_{\Omega^N}$ for scalar functions) the restriction operators, applied to vector functions defined in Ω, to the mesh Ω^N, and by $[\mathbf{v}]_{\partial\Omega^N}$ (analogously $[v]_{\partial\Omega^N}$ for scalar functions) the restriction operators, applied to vector functions defined in $\partial\Omega$, to the mesh $\partial\Omega^N$. For all $(x_i, y_j) \in \Omega^N$ we define the semidiscrete approach $\mathbf{U}^N(t) \equiv \mathbf{U}^N_{ij}(t)$, $i, j = 1, \ldots, N-1$, with $\mathbf{U}^N_{ij}(t) \approx \mathbf{u}(x_i, y_j, t)$, as the solution of the Initial Value Problem

$$\begin{cases} \tilde{\mathcal{L}}^N_\varepsilon(t)\overline{\mathbf{U}}^N(t) \equiv \dfrac{d\mathbf{U}^N(t)}{dt} + \mathcal{L}^N_\varepsilon(t)\overline{\mathbf{U}}^N(t) = [\mathbf{f}(\mathbf{x},t)]_{\Omega^N}, \text{ in } \Omega^N \times [0,T], \\ \overline{\mathbf{U}}^N(t) = [\mathbf{g}(\mathbf{x},t)]_{\Gamma^N}, \text{in } \partial\Omega^N \times [0,T], \\ \mathbf{U}^N(0) = [\boldsymbol{\varphi}(\mathbf{x})]_{\Omega^N}, \end{cases} \tag{22}$$

being $\overline{\mathbf{U}}^N(t)$ the natural extension of the semidiscrete functions $\mathbf{U}^N(t)$, defined in $\Omega^N \times [0,T]$, to $\overline{\Omega}^N \times [0,T]$ by adding the Dirichlet boundary values of $\mathbf{g}$ in $\partial\Omega^N \times [0,T]$ and being $\mathcal{L}^N_\varepsilon(t)$ the discretization, via the classical upwind scheme differences, of the convection-diffusion operator $\mathcal{L}_{\mathbf{x},\varepsilon}(t)$, i.e.,

$$\begin{aligned} &(\mathcal{L}^N_\varepsilon(t)\overline{\mathbf{U}}^N(t))_{ij,1} = c_{ij,l_1}U^N_{i-1j,1} + c_{ij,r_1}U^N_{i+1j,1} + c_{ij,d_1}U^N_{ij-1,1} + c_{ij,u_1}U^N_{ij+1,1} + \\ &c_{ij,c_1}U^N_{ij,1} + a_{11}(t)U^N_{ij,1} + a_{12}(t)U^N_{ij,2}, \end{aligned} \tag{23}$$

where the coefficients c_{ij} are given by

$$\begin{aligned} &c_{ij,l_1} = \frac{-\varepsilon_1}{h_{x,i}\overline{h}_{x,i}} - \frac{b_{11}(x_i,y_j)}{h_{x,i}}, c_{ij,r_1} = \frac{-\varepsilon_1}{h_{x,i+1}\overline{h}_{x,i}}, c_{ij,d_1} = \frac{-\varepsilon_1}{h_{y,j}\overline{h}_{y,j}} - \frac{b_{21}(x_i,y_j)}{h_{y,j}}, \\ &c_{ij,u_1} = \frac{-\varepsilon_1}{h_{y,j+1}\overline{h}_{y,j}}, \quad c_{ij,c_1} = -(c_{ij,l_1} + c_{ij,r_1} + c_{ij,d_1} + c_{ij,u_1}), \end{aligned} \tag{24}$$

and

$$\begin{aligned} &(\mathcal{L}^N_\varepsilon(t)\overline{\mathbf{U}}^N(t))_{ij,2} = c_{ij,l_2}U^N_{i-1j,2} + c_{ij,r_2}U^N_{i+1j,2} + c_{ij,d_2}U^N_{ij-1,2} + c_{ij,u_2}U^N_{ij+1,2} + \\ &c_{ij,c_2}U^N_{ij,2} + a_{21}(t)U^N_{ij,1} + a_{22}(t)U^N_{ij,2}, \end{aligned} \tag{25}$$

and now the coefficients c_{ij} are given by

$$\begin{aligned} &c_{ij,l_2} = \frac{-\varepsilon_2}{h_{x,i}\overline{h}_{x,i}} - \frac{b_{12}(x_i,y_j)}{h_{x,i}}, c_{ij,r_2} = \frac{-\varepsilon_2}{h_{x,i+1}\overline{h}_{x,i}}, c_{ij,d_2} = \frac{-\varepsilon_2}{h_{y,j}\overline{h}_{y,j}} - \frac{b_{22}(x_i,y_j)}{h_{y,j}}, \\ &c_{ij,u_2} = \frac{-\varepsilon_2}{h_{y,j+1}\overline{h}_{y,j}}, \quad c_{ij,c_2} = -(c_{ij,l_2} + c_{ij,r_2} + c_{ij,d_2} + c_{ij,u_2}), \end{aligned} \tag{26}$$

for $i, j = 1, \ldots, N-1$.

Lemma 7 *(Semidiscrete maximum principle). Let $(\tilde{\mathcal{L}}^N_\varepsilon(t)\overline{\mathbf{U}}^N(t))_{ij,k}, k = 1,2$, be the semidiscrete operator given in (22)-(26) and let be $\boldsymbol{\Psi}(t)$ a semidiscrete grid function. If $\boldsymbol{\Psi}(x_i,y_j,t) \geq \mathbf{0}$ on $\Gamma^N \times [0,T]$ and $(\tilde{\mathcal{L}}^N_\varepsilon(t)\boldsymbol{\Psi}(x_i,y_j,t))_{ij,k} \geq \mathbf{0}, k = 1,2, \ \forall (x_i,y_j,t) \in \Omega^N \times [0,T]$, then it holds $\boldsymbol{\Psi}(x_i,y_j,t) \geq \mathbf{0}, \ \forall (x_i,y_j,t) \in \overline{\Omega}^N \times [0,T]$.*

Proof. The proof follows literately the ideas given in [8,16], and therefore we think that it is not necessary to include the details. □

Lemma 8 *(Discrete stability result). Let $\mathbf{U}^N(t)$ be the solution of (22). Then, it holds*

$$\|\mathbf{U}^N(t)\|_{\overline{\Omega}^N \times [0,T]} \leq \frac{1}{\beta}\|\frac{d\mathbf{U}^N}{dt}(t) + \mathcal{L}^N_\varepsilon(t)\overline{\mathbf{U}}^N(t)\|_{\Omega^N \times [0,T]} + \|\mathbf{U}^N(t)\|_{\Gamma^N \times [0,T]}.$$

Proof. To prove the stability, we consider the barrier functions $\boldsymbol{\Psi}_\pm(t)$, which are defined by

$$\boldsymbol{\Psi}_{k,\pm}(x_i,y_j,t) = \frac{x_i}{\beta}\|\frac{d\mathbf{U}^N}{dt}(t) + \mathcal{L}^N_\varepsilon(t)\overline{\mathbf{U}}^N(t)\|_{\Omega^N \times [0,T]} + \|\mathbf{U}^N(t)\|_{\Gamma^N \times [0,T]} \pm \mathbf{U}^N_{ij,k}(t).$$

Then, clearly it holds $\boldsymbol{\Psi}_{k,\pm}(x_i,y_j,t) \geq \mathbf{0}$ on $\Gamma^N \times [0,T]$ and $(\tilde{\mathcal{L}}^N_\varepsilon(t)\boldsymbol{\Psi}_\pm(t))_{ij,k} \geq \mathbf{0}, k = 1,2, \ \forall (x_i,y_j,t) \in \Omega^N \times [0,T]$; applying now Lemma 7, the result immediately follows. □

To prove the uniform convergence of the method, following to the continuous problem, we decompose the numerical solution in the form

$$\mathbf{U}^N(t) = \mathbf{V}^N(t) + \mathbf{W}^N_r(t) + \mathbf{W}^N_t(t) + \mathbf{P}^N_{rt}(t), \tag{27}$$

where the regular component is the solution of the semidiscrete problem

$$\begin{cases} \tilde{\mathcal{L}}_{\varepsilon}^{N}(t)\overline{\mathbf{V}}^{N}(t) = [\mathbf{f}(\mathbf{x},t)]_{\Omega^N}, \text{ in } \Omega^N \times [0,T], \\ \overline{\mathbf{V}}^{N}(t) = \psi_1(y), \quad \forall (x,y,t) \in \Gamma_1^N \times [0,T], \\ \overline{\mathbf{V}}^{N}(t) = \psi_2(x), \quad \forall (x,y,t) \in \Gamma_2^N \times [0,T], \\ \overline{\mathbf{V}}^{N}(t) = \psi_3(y), \quad \forall (x,y,t) \in \Gamma_3^N \times [0,T], \\ \overline{\mathbf{V}}^{N}(t) = \psi_4(x), \quad \forall (x,y,t) \in \Gamma_4^N \times [0,T], \\ \mathbf{V}^{N}(0) = [\boldsymbol{\varphi}(\mathbf{x})]_{\Omega^N}, \end{cases} \tag{28}$$

the boundary layer component is the solution of the semidiscrete problem

$$\begin{cases} \tilde{\mathcal{L}}_{\varepsilon}^{N}(t)\overline{\mathbf{W}}_{k}^{N}(t) = \mathbf{0}, \text{ in } \Omega^N \times [0,T], \ k = r,t, \\ \overline{\mathbf{W}}_{r}^{N}(t) = (\overline{\mathbf{U}}^{N}(t) - \overline{\mathbf{V}}^{N}(t)), \forall (x,y) \in \Gamma_3^N, \\ \overline{\mathbf{W}}_{r}^{N}(t) = 0, \forall (x,y) \in \Gamma_1^N \cup \Gamma_2^N \cup \Gamma_4^N, \\ \overline{\mathbf{W}}_{t}^{N}(t) = (\overline{\mathbf{U}}^{N}(t) - \overline{\mathbf{V}}^{N}(t)), \forall (x,y) \in \Gamma_4^N, \\ \overline{\mathbf{W}}_{t}^{N}(t) = 0, \forall (x,y) \in \Gamma_1^N \cup \Gamma_2^N \cup \Gamma_3^N, \\ \mathbf{W}_{k}^{N}(0) = \mathbf{0}, \text{ in } \Omega^N, \quad k = r,t, \end{cases} \tag{29}$$

and finally, the corner layer component is the solution of the semidiscrete problem

$$\begin{cases} \tilde{\mathcal{L}}_{\varepsilon}^{N}(t)\overline{\mathbf{P}}_{rt}^{N}(t) = \mathbf{0}, \text{ in } \Omega^N \times [0,T], \\ \overline{\mathbf{P}}_{rt}^{N}(t) = -\overline{\mathbf{W}}_{r}^{N}(t), \ \forall (x,y) \in \Gamma_3^N, \\ \overline{\mathbf{P}}_{rt}^{N}(t) = -\overline{\mathbf{W}}_{t}^{N}(t), \ \forall (x,y) \in \Gamma_4^N, \\ \overline{\mathbf{P}}_{rt}^{N}(t) = \mathbf{0}, \ \forall (x,y) \in \Gamma_1^N \cup \Gamma_2^N, \\ \mathbf{P}_{rt}^{N}(0) = \mathbf{0}, \text{ in } \Omega^N. \end{cases} \tag{30}$$

Theorem 1. *The global error $e_N(x_i,y_j,t) = u(x_i,y_j,t) - U^N(x_i,y_j)(t)$, associated to the spatial discretization (22)-(26), defined on the adequate Shishkin mesh given by (20), satisfies*

$$\|e_N(x_i,y_j,t)\|_{\overline{\Omega}_N} \leq CN^{-1}\ln N, \quad \forall\, t \in [0,T]. \tag{31}$$

Therefore, the solution of the spatial semidiscrete problem (22) converges uniformly to the solution of (1) with almost first order of convergence.

Proof. We follow the technique used in [14], where an elliptic coupled system of convection-diffusion type with different diffusion parameters and also a parameter in the convection term, was analyzed. Here, we include the minimum details to understand the proof.

Based on the previous decompositions for the exact and the numerical solutions, to bound the error, we must study the error associated to each component separately. Note that the local error of the numerical scheme depends only of the spatial discretization.

First, for the regular component, using standard Taylor expansions, the local error satisfies

$$\begin{aligned} &\left|\mathcal{L}_{\varepsilon}^{N}(t)\left(\mathbf{V}^{N}(t) - [\mathbf{v}]_{\Omega^N}\right)\right| \leq \\ &C\left[(h_{x,i}+h_{x,i+1})\left(\varepsilon\left\|\frac{\partial^3\mathbf{v}}{\partial x^3}\right\| + \left\|\frac{\partial^2\mathbf{v}}{\partial x^2}\right\|\right) + (h_{y,j}+h_{y,j+1})\left(\varepsilon\left\|\frac{\partial^3\mathbf{v}}{\partial y^3}\right\| + \left\|\frac{\partial^2\mathbf{v}}{\partial y^2}\right\|\right)\right], \end{aligned} \tag{32}$$

and therefore, it is straightforward to prove that it holds

$$\left|\mathcal{L}_{\varepsilon}^{N}(t)\left(\mathbf{V}^{N}(t) - [\mathbf{v}]_{\Omega^N}\right)\right| \leq CN^{-1}.$$

Using Lemma 7, we can deduce

$$|\mathbf{v}(x_i,y_j,t) - \mathbf{V}^{N}(x_i,y_j)(t)| \leq CN^{-1}. \tag{33}$$

In second place we study the error associated to the layer components; we only show the details for $\mathbf{w}_r$ and similarly we can proceed for $\mathbf{w}_t$. As it is usual, we use the barrier functions technique. To do that, we define the functions

$$\mathcal{B}_1^{r,N}(x_i) = \prod_{l=i+1}^{N}\left(1+\frac{\beta h_l}{2\varepsilon_1}\right)^{-1}, \qquad \mathcal{B}_2^{r,N}(x_i) = \prod_{l=i+1}^{N}\left(1+\frac{\beta h_l}{2\varepsilon_2}\right)^{-1},$$

with $\mathcal{B}_1^{r,N}(x_N) = \mathcal{B}_2^{r,N}(x_N) = 1$, and also

$$\mathcal{B}_1^{t,N}(y_j)=\prod_{l=j+1}^{N}\left(1+\frac{\beta h_l}{2\varepsilon_1}\right)^{-1},\qquad \mathcal{B}_2^{t,N}(y_j)=\prod_{l=j+1}^{N}\left(1+\frac{\beta h_l}{2\varepsilon_2}\right)^{-1},$$

with $\mathcal{B}_1^{t,N}(x_N)=\mathcal{B}_2^{t,N}(x_N)=1$. Then, it is well known that it holds

$$|W_{r_1}^N(x_i,y_j,t)|\le C\mathcal{B}_2^{r,N}(x_i),\quad |W_{r_2}^N(x_i,y_j,t)|\le C\mathcal{B}_2^{r,N}(x_i),$$

and also that

$$|W_{t_1}^N(x_i,y_j,t)|\le C\mathcal{B}_2^{t,N}(y_j),\quad |W_{t_2}^N(x_i,y_j,t)|\le C\mathcal{B}_2^{t,N}(y_j).$$

To bound the local error we use (32) changing $\mathbf{v}$ by $\mathbf{w}_r$. Then, we distinguish several cases. First, when the mesh is uniform, a detailed analysis (see [14]), permits us to obtain that it holds

$$|(\mathbf{W}_r^N-\mathbf{w}_r)(x_i,y_j,t)|\le CN^{-1}\begin{pmatrix}\varepsilon_1^{-1}+\varepsilon_2^{-1}\\ \varepsilon_1^{-1}\end{pmatrix},$$

and taking into account that if the mesh is uniform, then it holds $\varepsilon_k\ln N\ge C,\ k=1,2$, i.e., $\varepsilon_k^{-1}\le C\ln N,\ k=1,2$ and it follows

$$|(\mathbf{W}_r^N-\mathbf{w}_r)(x_i,y_j,t)|\le CN^{-1}\ln N.$$

On the other hand, when $\sigma_2=\sigma_0\varepsilon_2\ln N$, for $0\le j\le N,\ 0\le i\le 3N/4$, we can obtain

$$\begin{aligned}&|(W_{r_1}^N-w_{r_1})(x_i,y_j,t)|\le |W_{r_1}^N(x_i,y_j,t)|+|w_{r_1}(x_i,y_j,t)|\le C\mathcal{B}_2^{r,N}(x_i)+C\mathcal{B}_2^{r,N}(x_i)\\ &\le C\mathcal{B}_2^{r,N}(1-\sigma_2)+C\mathcal{B}_2^{r,N}(1-\sigma_2)\le CN^{-1},\end{aligned}$$

and analogously we can obtain

$$|(W_{r_2}^N-w_{r_2})(x_i,y_j,t)|\le CN^{-1}.$$

In the other case, i.e., for $0\le j\le N,\ 3N/4\le i\le N$, it can be proved that

$$|(W_{r_k}^N-w_{r_k})(x_i,y_j,t)|\le CN^{-1}\ln N,\quad k=1,2.$$

The last case is when $\sigma_2=1/4$ and $\sigma_1=\sigma_0\varepsilon_1\ln N$; then, following to [14], again it can be proved that

$$|(W_{r_k}^N-w_{r_k})(x_i,y_j,t)|\le CN^{-1}\ln N,\quad k=1,2.$$

Finally, we study the error associated to the corner layer component. Again, we use (32) changing $\mathbf{v}$ by $\mathbf{p}_{rt}$ and we distinguish several cases. First, when the mesh is uniform, we have

$$|(\mathbf{P}_{rt}^N-\mathbf{p}_r)(x_i,y_j,t)|\le CN^{-1}\begin{pmatrix}\varepsilon_1^{-1}+\varepsilon_2^{-1}\\ \varepsilon_1^{-1}\end{pmatrix},$$

and taking into account that if the mesh is uniform, then it holds $\varepsilon_k\ln N\ge C,\ k=1,2$, i.e., $\varepsilon_k^{-1}\le C\ln N,\ k=1,2$ and it follows

$$|(\mathbf{P}_{rt}^N-\mathbf{p}_{rt})(x_i,y_j,t)|\le CN^{-1}\ln N.$$

Next, when $\sigma_2=\sigma_0\varepsilon_2\ln N$, for the grid points $\{(x_i,y_j),|\,0\le i,j\ <3N/4\}$, it holds

$$\begin{aligned}&|(P_{rt_1}^N-p_{rt_1})(x_i,y_j,t)|\le |P_{rt_1}^N(x_i,y_j,t)|+|p_{rt_1}(x_i,y_j,t)|\le C\mathcal{B}_2^{r,N}(x_i)+C\mathcal{B}_2^{t,N}(y_j)\\ &\le C\mathcal{B}_2^{r,N}(1-\sigma_2)+C\mathcal{B}_2^{t,N}(1-\sigma_2)\le CN^{-1},\end{aligned}$$

and analogously we can prove

$$|(P_{rt_2}^N-p_{rt_2})(x_i,y_j,t)|\le CN^{-1}.$$

In the other case, i.e., for $3N/4\le i,j\le N$, it can be proved that

$$|(P_{rt_k}^N-p_{rt_k})(x_i,y_j,t)|\le CN^{-1}\ln N,\quad k=1,2.$$

The last case is when $\sigma_2=1/4$ and $\sigma_1=\sigma_0\varepsilon_1\ln N$; then, following to [14], again it can be proved that

$$|(P_{rt_k}^N-p_{rt_k})(x_i,y_j,t)|\le CN^{-1}\ln N,\quad k=1,2.$$

From all previous estimates for the errors associated to the regular, boundary layer and corner components, respectively, the required result follows. □

4. The fully discrete scheme: uniform convergence

In this section we construct the fully discrete scheme which we propose to solve the continuous (1). To complete the discretization process, we apply an adequate time integrator to the semidiscrete problems (22). This process follows the same ideas as the developed ones in [11], where two dimensional parabolic reaction-diffusion systems were considered.

To simplify the notations of the algorithm, it is usual structure the semidiscrete solution by blocks in the form $\overline{\mathbf{U}}(t_m)^N \equiv ((U_{ij,1}(t_m)),(U_{ij,2}(t_m)))$; also, it is very common in the literature introduce the three point difference operators

$$\begin{array}{l}\mathcal{L}^N_{1,x}(t)v^N \equiv -\varepsilon_1\partial_{xx}v^N + b_{11}\partial_{\bar{x}}v^N + a_{11,x}(t)v^N,\\ \mathcal{L}^N_{1,y}(t)v^N \equiv -\varepsilon_1\partial_{yy}v^N + b_{12}\partial_{\bar{y}}v^N + a_{11,y}(t)v^N,\\ \mathcal{L}^N_{2,x}(t)v^N \equiv -\varepsilon_2\partial_{xx}v^N + b_{21}\partial_{\bar{x}}v^N + a_{22,x}(t)v^N,\\ \mathcal{L}^N_{2,y}(t)v^N \equiv -\varepsilon_2\partial_{yy}v^N + b_{22}\partial_{\bar{y}}v^N + a_{22,y}(t)v^N,\end{array} \tag{34}$$

being ∂_{xx} and ∂_{yy} the classical second order central difference operator and $\partial_{\bar{x}},\ \partial_{\bar{y}}$ are the discretization via backward differences of the first derivatives in (1), on the rectangular Shishkin mesh introduced in previous section. As well, we consider here a splitting of the diagonal reaction coefficients in the form $a_{rr,x}(x,y,t)+a_{rr,y}(x,y,t)=a_{rr}(x,y,t), r=1,2$ preserving the positivity of their addends, i.e. $a_{rr,z}(x,y,t)\geq 0,\ r=1,2, z=x,y$. To include the contribution of the non diagonal reaction coefficients, which are responsible of the coupling of the system, we extend the three point difference operators of (34) to

$$L^N_{\varepsilon,1}(t_{m+1}) \equiv \begin{pmatrix} \mathcal{L}^N_{1,x}(t_{m+1}) & a_{12,x}(t_{m+1}) \\ 0 & 0 \end{pmatrix},\ L^N_{\varepsilon,2}(t_{m+1}) \equiv \begin{pmatrix} 0 & 0 \\ a_{21,x}(t_{m+1}) & \mathcal{L}^N_{2,x}(t_{m+1}) \end{pmatrix},$$
$$L^N_{\varepsilon,3}(t_{m+1}) \equiv \begin{pmatrix} 0 & 0 \\ a_{21,y}(t_{m+1}) & \mathcal{L}^N_{2,y}(t_{m+1}) \end{pmatrix},\ L^N_{\varepsilon,4}(t_{m+1}) \equiv \begin{pmatrix} \mathcal{L}^N_{1,y}(t_{m+1}) & a_{12,y}(t_{m+1}) \\ 0 & 0 \end{pmatrix}.$$

Notation $a_{rp,z}(t)v^N$ must be understood as follows: $(a_{rp,z}(t)v^N)_{ij} \equiv a_{rp,z}(x_i,y_j,t)v^N_{ij}$. Analogously to the diagonal terms, here we have split the non diagonal coefficients of the reaction matrix in the form $a_{rp,x}(x,y,t)+a_{rp,y}(x,y,t)=a_{rp}(x,y,t),\ r,p=1,2, r\neq p$; the only restrictions to this partition are $a_{rp,z}(x,y,t)\leq 0,\ r,p=1,2, r\neq p, z=x,y$, and $\sum_{p=1}^{2} a_{rp,z}(x,y,t)\geq 0, r=1,2, z=x,y$.

Moreover, we decompose the source term $\mathbf{f}(\mathbf{x},t)\equiv(f_1,f_2)^T$, in the form $\mathbf{f}_x+\mathbf{f}_y \equiv (f_{1,x},f_{2,x})^T+(f_{1,y},f_{2,y})^T$ and we denote $F^N_{1,x},F^N_{2,x},F^N_{1,y},F^N_{2,x}$ to the vectors which contain the evaluations of these terms at the grid points. As any of these four source terms are involved only in one block of the system, we extend such terms to the whole dimension of the system by adding a block of zeros in the corresponding place as follows:

$$\mathbf{F}^{N,m+1/4} \equiv \begin{pmatrix} F^N_{1,x}(t_{m+1}) \\ 0 \end{pmatrix}, \mathbf{F}^{N,m+2/4} \equiv \begin{pmatrix} 0 \\ F^N_{2,x}(t_{m+1}) \end{pmatrix},$$
$$\mathbf{F}^{N,m+3/4} \equiv \begin{pmatrix} 0 \\ F^N_{2,y}(t_{m+1}) \end{pmatrix},\ \mathbf{F}^{N,m+1} \equiv \begin{pmatrix} F^N_{1,y}(t_{m+1}) \\ 0, \end{pmatrix}.$$

Using the previous notations, we are in disposition of define our fully discrete method. Let $\tau \equiv T/M$ be the time step, $t_m = m\tau, m=0,\ldots,M$ are the intermediate times where the semidiscrete solution $\overline{\mathbf{U}}^N(t_m)$ is going to be approached by $\mathbf{U}^{N,m}$. Let us denote $\Omega^N_1 \equiv \Omega^N_3 \equiv I^N_x \times \overline{I}^N_y$, $\Omega^N_2 \equiv \Omega^N_4 \equiv \overline{I}^N_x \times I^N_y$, $\partial\Omega^N_1 \equiv \partial\Omega^N_2 \equiv \Gamma^N_1 \bigcup \Gamma^N_3$, $\partial\Omega^N_3 \equiv \partial\Omega^N_4 \equiv \Gamma^N_2 \bigcup \Gamma^N_4$. Then, the fully discrete scheme is given by

$$\begin{array}{l}\text{(initialize)}\ \ \mathbf{U}^{N,0} = [\boldsymbol{\varphi}]_{\overline{\Omega}^N},\\ \left\{\begin{array}{l}\left\{\begin{array}{l}\text{(calculus of } \mathbf{U}^{N,m+1}),\\ (I+\tau L^N_{\varepsilon,l}(t_{m+1}))\mathbf{U}^{N,m+l/4} = \mathbf{U}^{N,m+(l-1)/4} + \tau\mathbf{F}^{N,m+l/4},\ \ \text{in } \Omega^N_l,\\ \mathbf{U}^{N,m+l/4} = \mathbf{G}^{N,m+l/4}, \text{in } \partial\Omega^N_l,\\ l=1,2,3,4,\end{array}\right.\\ m=0,\ldots,M-1,\end{array}\right.\end{array} \tag{35}$$

where the boundary data are given by

$$\begin{array}{l}\mathbf{G}^{N,m+1/4} = \Big([(I+\tau\mathcal{L}^N_{1,y}(t_{m+1}))[g_1(\mathbf{x},t_{m+1})]_{\Omega_N}]_{\partial\Omega^N_1} - \tau[f_{1,y}(\mathbf{x},t_{m+1})]_{\partial\Omega^N_1} +\\ [\tau a_{12,y}(\mathbf{x},t_{m+1})g_2(\mathbf{x},t_{m+1})]_{\partial\Omega^N_1}, [U^{N,m}_2]_{\partial\Omega^N_1}\Big)\\ \mathbf{G}^{N,m+1/2} = \Big([U^{N,m+1/4}_1]_{\partial\Omega^N_2}, [(I+\tau\mathcal{L}^N_{2,y}(t_{m+1}))[g_2(\mathbf{x},t_{m+1})]_{\Omega_N}]_{\partial\Omega^N_2} -\\ \tau[f_{2,y}(\mathbf{x},t_{m+1})]_{\partial\Omega^N_2} + [\tau a_{21,y}(\mathbf{x},t_{m+1})g_1(\mathbf{x},t_{m+1})]_{\partial\Omega^N_2}\Big)\\ \mathbf{G}^{N,m+3/4} = ([U^{N,m+1/2}_1]_{\partial\Omega^N_3}, [g_2(\mathbf{x},t_{m+1})]_{\partial\Omega^N_3}) \text{ and}\\ \mathbf{G}^{N,m+1} = ([g_1(\mathbf{x},t_{m+1})]_{\partial\Omega^N_4}, [U^{N,m+3/4}_2]_{\partial\Omega^N_4}).\end{array} \tag{36}$$

Let us remark that in the calculus of the fractional stages $\mathbf{U}^{N,m+1/4}, \mathbf{U}^{N,m+1}$ of (35), their second blocks of unknowns remain unchanged with respect to the second block of the previous fractional step, while the first blocks of unknowns are computed by solving only tridiagonal linear systems; The opposite happens with respect to the blocks in the second and third fractional steps. Because of this, the computational cost of advancing one step in time with our algorithm is similar to the cost of any one step explicit method. If the implicit Euler method was chosen to integrate in time, for example, then a complicated block tridiagonal system should be solved at each time step to advance in time. Thus, we obtain a remarkable cost reduction with our method when we compare it with the uniformly convergent methods considered in previous papers.

In regard to the boundary data, we want to emphasize that our proposal improves the accuracy given by the following simpler and apparently natural choice

$$\mathbf{G}^{N,m+l/4} = [\mathbf{g}(\mathbf{x}, t_{m+1})]_{\partial\Omega_l^N},\ l = 1, 2, 3, 4. \tag{37}$$

In [11], both theoretical and practical reasons were given in a system of diffusion-reaction type to state that our choice for the boundary data is better than (37). This idea, to discretize the boundary conditions associated to singularly perturbed problems in that form, was first used in [6].

Let us state next the main theoretical properties of our algorithm. For the sake of shortness, we omit the proofs of the next assertions in this section because they are similar to their corresponding ones which we proved in [11].

Lemma 9. *(Inverse positivity of (35)). If all of the data ($\mathbf{G}^{N,m+l/4}, \mathbf{F}^{N,m+l/4}, [\boldsymbol{\varphi}]_{\Omega^N}$), which take part of (35), have non-negative components, then the solution $\mathbf{U}^{N,m},\ m = 1, \ldots, M$ of (35) has non-negative components.*

The proof of this result can be done, for example, by taking into account that the linear systems involved in (35) have inverse positive M-matrices where, besides, the sum of the coefficients of all of their rows is always ≥ 1. From this fact, it is not difficult to prove the next result.

Corollary 1. *(Contractivity of (35)). Two solutions $\mathbf{U}^{N,m+1}$ and $\tilde{\mathbf{U}}^{N,m+1}$ obtained with (35) from two different initial conditions $[\boldsymbol{\varphi}]_{\overline{\Omega}^N}$ and $[\tilde{\boldsymbol{\varphi}}]_{\overline{\Omega}^N}$ respectively satisfy*

$$\|\mathbf{U}^{N,m+1} - \tilde{\mathbf{U}}^{N,m+1}\|_{\Omega_N} \leq \|\mathbf{U}^{N,m} - \tilde{\mathbf{U}}^{N,m}\|_{\Omega_N},\ m = 0, 1, \ldots, M-1. \tag{38}$$

This contractivity result ensures the numerical stability of our proposal; to complete the numerical analysis of it, we now focus our attention on its uniform consistency. Thus, the concept of local error in time at time $t_{m+1},\ m = 0, \ldots, M-1$, is introduced as usual

$$\mathbf{e}^{N,m+1} \equiv \overline{\mathbf{U}}^N(t_{m+1}) - \widehat{\mathbf{U}}^{N,m+1}, \tag{39}$$

being $\widehat{\mathbf{U}}^{N,m+1}$ the result given by the step m of scheme (35) if we change $\mathbf{U}^{N,m}$ by $\overline{\mathbf{U}}^N(t_m)$.

Theorem 2. *(Uniform consistency of the time integrator). Under the assumptions (3)-(5), it holds*

$$\|\mathbf{e}^{N,m+1}\|_{\overline{\Omega}_N} \leq CM^{-2}, \quad \forall\ \tau\ \in (0, \tau_0]\ \text{ and } \forall\ m = 0, 1, \ldots, M-1. \tag{40}$$

Proof. The proof of this theorem follows the same scheme as our proof of Theorem 6 in [11]. □

The final step is to prove the uniform and the unconditional convergence of the time integration process. Then, we introduce the global error at time t_m, for $m = 1, \ldots, M$, as

$$\overline{\mathbf{U}}^N(t_m) - \mathbf{U}^{N,m},$$

and a classical and standard reasoning "*consistency + stability ⇒ convergence*" permits us to prove that the time integration process is uniformly convergent of first order, i.e.,

$$\|\overline{\mathbf{U}}^N(t_m) - \mathbf{U}^{N,m}\|_{\overline{\Omega}^N} \leq CM^{-1}, \tag{41}$$

being C independent of N, M, ε_1 and ε_2.

Finally, combining the results given in (31) and (41), it is straightforward to state and prove the main result of the paper.

Theorem 3. *(Uniform convergence). Assuming that (3)-(5) hold, the global error associated to the numerical method defined by (35) on the Shishkin mesh given in (20), satisfies*

$$\max_{0 \leq m \leq M} \|[\mathbf{u}(\mathbf{x}, t_m)]_{\overline{\Omega}^N} - \mathbf{U}^{N,m}\|_{\overline{\Omega}^N} \leq C\left(N^{-1} \ln N + M^{-1}\right) \tag{42}$$

being C independent of N, M ε_1 and ε_2; therefore, the numerical scheme (35) is uniformly convergent of first order in time and of almost first order in space.

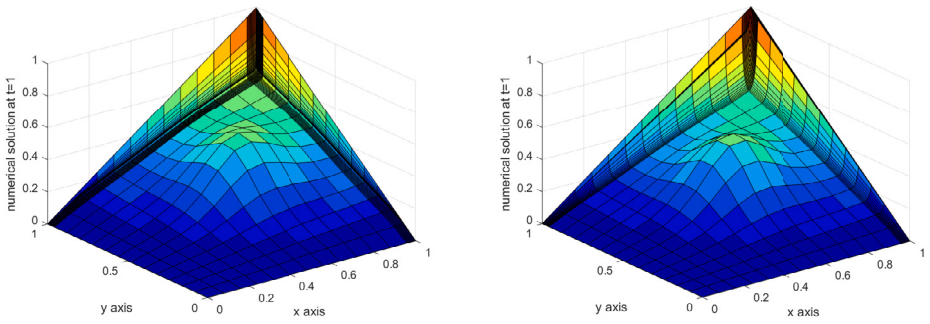

Fig. 1. Components u_1 (left) and u_2 (right) at $t = 1$ for $\varepsilon_1 = 10^{-4},\ \varepsilon_2 = 10^{-2}$ with $N = 36, M = 32$ for problem (43). (For interpretation of the colors in the figure(s), the reader is referred to the web version of this article.)

5. Numerical results

In this section, the numerical results obtained with our algorithm for some test problems of type (1) are shown; all of these computations have been performed in a PC with an Intel(R) Core(TM) i7-10700 running at @ 2.90 GH, using only one core, and programming in GNU Fortran with optimization-O2. The tridiagonal linear systems which are required to compute the numerical approximations at each time level, have been solved by using our own implementation of the classical Thomas's algorithm.

In all of the examples of this section, the constant σ_0 which appears in the definition of the transition parameters given in (21) and (49), has been chosen as $\sigma_0 = 1.2$.

The data of the first test problem are the following:

$$\begin{array}{l} T = 1, \\ b_{11}(x,y) = b_{12}(x,y) = b_{21}(x,y) = b_{22}(x,y) = 1, \\ a_{11}(x,y,t) = 10,\ a_{12}(x,y,t) = -10(2^{16})x^4(1-x)^4y^4(1-y)^4, \\ a_{21}(x,y,t) = -20(2^{16})x^4(1-x)^4y^4(1-y)^4, 0,\ a_{22}(x,y,t) = 20, \\ f_1(x,y,t) = (1-e^{-5t})(x+y) + 5xy,\ f_2(x,y,t) = (1-e^{-10t})(x+y) + 10xy, \\ \boldsymbol{\varphi}(x) = (0,0)^T, \\ \mathbf{g}(\mathbf{x},t) = ((1-e^{-5t})xy, (1-e^{-10t})xy)^T,\ (\mathbf{x},t) \in \partial\Omega \times [0,1]. \end{array} \tag{43}$$

Fig. 1 displays the numerical solution at $t = 1$ with $N = 36, M = 32,\ \varepsilon_1 = 10^{-4}$ and $\varepsilon_2 = 10^{-2}$. From it, we clearly see the boundary layers at the outflow boundary of the spatial domain. As the exact solution of this problem is unknown, to approximate the maximum errors for each component $u_k, k = 1, 2$, we use the double-mesh principle (see [18]), which permits to estimate the maximum errors as follows:

$$d_{\varepsilon,k}^{N,M} = \max_{0\le m\le M} \max_{0\le i,j\le N} |U_{N,i,j,k}^m - \widehat{U}_{2N,2i,2j,k}^{2m}|,\ d_k^{N,M} = \max_{\varepsilon} d_{\varepsilon,k}^{N,M}, k = 1, 2. \tag{44}$$

Here, $\{\widehat{\mathbf{U}}_{2N,i,j}^m\}$ is the numerical solution obtained using a finer mesh $\{(\hat{x}_i, \hat{y}_j, \hat{t}_m)\}$ which has the mesh points of the coarse meshes $\overline{I}_x^N$, $\overline{I}_y^N$ and their midpoints and halving the size of the time steps. From these approximated errors we obtain in a usual way the corresponding approximated orders of convergence; then, the approximated orders of convergence are obtained by

$$p_k^{N,M} = \log(d_{\varepsilon,k}^{N,M}/d_{\varepsilon,k}^{2N,2M})/\log 2,\ p_k^{uni} = \log(d_k^{N,M}/d_k^{2N,2M})/\log 2, k = 1, 2. \tag{45}$$

Tables 1 and 2 show the maximum errors and their corresponding orders of convergence for first and second component respectively, for some values of diffusion parameter ε_2, when ε_1 vary in the range $R = \{\varepsilon_1; \varepsilon_1 = \varepsilon_2, 2^{-2}\varepsilon_2, \ldots, 2^{-26}\}$ and for different values of the discretization parameters N and M. From them, we clearly observe the almost first order of uniform convergence in agreement with the theoretical results.

In this first example, we have chosen a problem according to the model (1) where the coefficients of the convection matrices depend only of the spatial variables; in this model problem we have omitted the time dependence in these coefficients in order to simplify the details associated to the asymptotic behavior of the exact solution of the continuous problem and the uniform convergence analysis of the numerical method. Nevertheless, the same results hold in the cases where the convective coefficients depend also on the time variable. To corroborate this fact in practice, we consider a second test problem whose data are given by

Table 1
Estimated maximum and uniform errors and orders of convergence for the component u_1 in problem (43).

ε_2	N = 18 M = 8	N = 36 M = 16	N = 72 M = 32	N = 144 M = 64	N = 288 M = 128
2^{-6}	5.0906E-2 0.3648	3.9533E-2 0.3747	3.0491E-2 0.5870	2.0298E-2 0.7395	1.2158E-2
2^{-8}	5.3188E-2 0.2648	4.4270E-2 0.4578	3.2233E-2 0.5441	2.2105E-2 0.7046	1.3564E-2
2^{-10}	5.3299E-2 0.2500	4.4819E-2 0.4398	3.3043E-2 0.5453	2.2642E-2 0.6990	1.3948E-2
2^{-12}	5.3280E-2 0.2470	4.4897E-2 0.4353	3.3202E-2 0.5437	2.2778E-2 0.6969	1.4052E-2
2^{-14}	5.3273E-2 0.2463	4.4912E-2 0.4343	3.3238E-2 0.5433	2.2808E-2 0.6960	1.4079E-2
2^{-16}	5.3271E-2 0.2461	4.4916E-2 0.4340	3.3247E-2 0.5432	2.2816E-2 0.6958	1.4086E-2
2^{-18}	5.3271E-2 0.2461	4.4917E-2 0.4340	3.3249E-2 0.5432	2.2817E-2 0.6957	1.4087E-2
2^{-20}	5.3270E-2 0.2461	4.4917E-2 0.4339	3.3249E-2 0.5432	2.2818E-2 0.6957	1.4088E-2
$d_1^{N,M}$ p_1^{uni}	5.3299E-2 0.2461	4.4917E-2 0.4339	3.3249E-2 0.5432	2.2818E-2 0.6957	1.4088E-2

Table 2
Estimated maximum and uniform errors and orders of convergence for the component u_2 in problem (43).

ε_2	N = 18 M = 8	N = 36 M = 16	N = 72 M = 32	N = 144 M = 64	N = 288 M = 128
2^{-6}	4.8747E-2 0.4135	3.6599E-2 0.5492	2.5012E-2 0.6733	1.5684E-2 0.7777	9.1488E-3
2^{-8}	4.9374E-2 0.3124	3.9760E-2 0.4672	2.8761E-2 0.6183	1.8736E-2 0.7162	1.1405E-2
2^{-10}	4.8930E-2 0.2876	4.0087E-2 0.4355	2.9642E-2 0.5809	1.9817E-2 0.7097	1.2118E-2
2^{-12}	4.8859E-2 0.2844	4.0118E-2 0.4245	2.9891E-2 0.5744	2.0074E-2 0.7079	1.2290E-2
2^{-14}	4.8839E-2 0.2836	4.0122E-2 0.4218	2.9950E-2 0.5728	2.0136E-2 0.7067	1.2338E-2
2^{-16}	4.8833E-2 0.2835	4.0123E-2 0.4212	2.9965E-2 0.5724	2.0152E-2 0.7062	1.2352E-2
2^{-18}	4.8832E-2 0.2834	4.0123E-2 0.4210	2.9968E-2 0.5723	2.0155E-2 0.7061	1.2355E-2
2^{-20}	4.8832E-2 0.2834	4.0123E-2 0.4209	2.9969E-2 0.5722	2.0156E-2 0.7060	1.2356E-2
$d_2^{N,M}$ p_2^{uni}	4.9374E-2 0.2993	4.0123E-2 0.4209	2.9969E-2 0.5722	2.0156E-2 0.7060	1.2356E-2

$$
\begin{aligned}
&T = 1,\\
&b_{11}(x,y,t) = (1+x^2y^2)(1+t),\ b_{12}(x,y,t) = (3-x-xy)\sin(t+1),\\
&b_{21}(x,y,t) = (3+xy)\sin(t+1),\ b_{22}(x,y,t) = (2-xy)(1+t),\\
&a_{11}(x,y,t) = (1+t)(x+y+1),\ a_{12}(x,y,t) = -(1+t)(x+y),\\
&a_{21}(x,y,t) = -(1-e^{-t})(x^2+y^2),\ a_{22}(x,y,t) = (1-e^{-t})(x^2+y^2+2),\\
&f_1(x,y,t) = 10t^2(1-5t\sin(x+y)),\ f_2(x,y,t) = 10t(1-e^{-t})\cos(xy),\\
&\boldsymbol{\varphi}(x) = (0,0)^T,\\
&\mathbf{g}(\mathbf{x},t) = (0,0)^T,\ (\mathbf{x},t) \in \partial\Omega \times [0,1].
\end{aligned}
\tag{46}
$$

Fig. 2 displays the numerical solution at $t = 1$ with $N = 36$, $M = 32$, $\varepsilon_1 = 10^{-3}$ and $\varepsilon_2 = 5 \times 10^{-2}$. From it, we can observe again boundary layers at the outflow boundary of the spatial domain. Tables 3 and 4 show the maximum errors and their corresponding

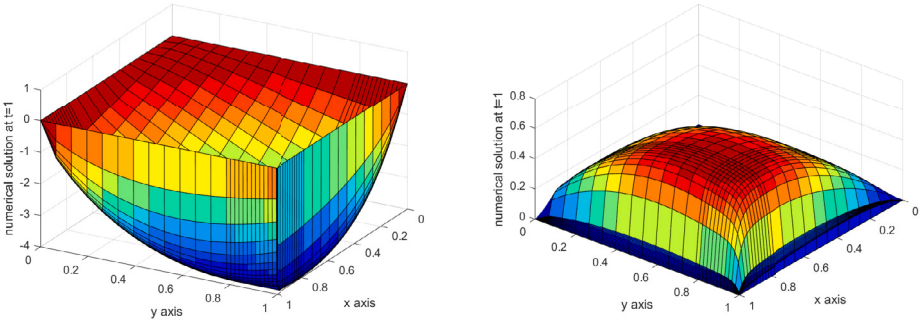

Fig. 2. Components u_1 (left) and u_2 (right) at $t = 1$ for $\varepsilon_1 = 10^{-3}$, $\varepsilon_2 = 5 \times 10^{-2}$ with $N = 36, M = 32$ for problem (46).

Table 3
Estimated maximum and uniform errors and orders of convergence for component u_1 in problem (46).

ε_2	N=18 M=8	N=36 M=16	N=72 M=32	N=144 M=64	N=288 M=128
2^{-6}	3.9209E-1 0.5223	2.7300E-1 0.6089	1.7901E-1 0.5693	1.2064E-1 0.6684	7.5908E-2
2^{-8}	4.0527E-1 0.5438	2.7800E-1 0.6400	1.7840E-1 0.5693	1.2023E-1 0.6831	7.4883E-2
2^{-10}	4.0915E-1 0.5493	2.7960E-1 0.6432	1.7903E-1 0.5757	1.2012E-1 0.6903	7.4446E-2
2^{-12}	4.1016E-1 0.5506	2.8002E-1 0.6439	1.7921E-1 0.5766	1.2017E-1 0.6931	7.4328E-2
2^{-14}	4.1041E-1 0.5510	2.8013E-1 0.6441	1.7926E-1 0.5768	1.2018E-1 0.6938	7.4299E-2
2^{-16}	4.1048E-1 0.5510	2.8016E-1 0.6441	1.7927E-1 0.5768	1.2019E-1 0.6938	7.4293E-2
2^{-18}	4.1049E-1 0.5511	2.8017E-1 0.6441	1.7927E-1 0.5769	1.2019E-1 0.6940	7.4291E-2
2^{-20}	4.1050E-1 0.5511	2.8017E-1 0.6441	1.7927E-1 0.5769	1.2019E-1 0.6940	7.4290E-2
$d_1^{N,M}$ p_1^{uni}	4.1050E-1 0.5511	2.8017E-1 0.6441	1.7927E-1 0.5714	1.2064E-1 0.6684	7.5908E-2

orders of convergence for first and second component respectively, for the same values of $\varepsilon_1, \varepsilon_2, N$ and M as in the first example. From them, the almost first order of uniform convergence appears again.

To show that our technique can be extended to larger systems, we consider a system with three components; in this case the data are given by

$$
\begin{aligned}
&\mathcal{A} = \begin{pmatrix} (1+t)e^{x+y} & -t(x+y) & -tx \\ -(x+y) & (1+t)(3+x+y) & -t\sin(y) \\ -xy^2 & -t(\sin(x)+\sin(y)) & e^t(2+\cos(x+y)) \end{pmatrix}, \\
&\mathcal{B}_1 = \begin{pmatrix} 1+xy/2 & 0 & 0 \\ 0 & 5+x^2y & 0 \\ 0 & 0 & 3-xy \end{pmatrix}, \\
&\mathcal{B}_2 = \begin{pmatrix} e^{x^2y} & 0 & 0 \\ 0 & 3+\sin(x+y)y & 0 \\ 0 & 0 & 1+x+y \end{pmatrix}, \\
&\mathbf{f}(\mathbf{x},t) = (-10(1-e^{-t})(x+y), 5t\sin(xy), 4(-1+e^t)\cos(x+y))^T, \\
&\mathbf{g}(\mathbf{x},t) \equiv (g_1,g_2,g_3)^T = \mathbf{0}, \ \boldsymbol{\varphi}(\mathbf{x}) = \mathbf{0},
\end{aligned}
\tag{47}
$$

and $T = 1$, for which again the exact solution is unknown. We solve this problem by using similar ideas to the used ones in the problem with only two components.

Firstly, to construct the appropriate piecewise uniform Shishkin mesh, we follow similar ideas to those ones in [30]. Now, we define $\overline{I}_x^N$ (and similarly for $\overline{I}_y^N$) as follows. Let N be multiple of 4; then, the grid points of $\bar{I}_x^N$ are given by

Table 4
Estimated maximum and uniform errors and orders of convergence for component u_2 in problem (46).

ε_2	N = 18 M = 8	N = 36 M = 16	N = 72 M = 32	N = 144 M = 64	N = 288 M = 128
2^{-6}	1.4902E-1 0.4104	1.1213E-1 0.4962	7.9493E-2 0.6123	5.2001E-2 0.6791	3.2477E-2
2^{-8}	1.5025E-1 0.3852	1.1504E-1 0.4917	8.1818E-2 0.5909	5.4322E-2 0.6466	3.4701E-2
2^{-10}	1.5115E-1 0.3848	1.1576E-1 0.4891	8.2476E-2 0.5859	5.4947E-2 0.6307	3.5489E-2
2^{-12}	1.5138E-1 0.3848	1.1594E-1 0.4877	8.2682E-2 0.5854	5.5104E-2 0.6261	3.5703E-2
2^{-14}	1.5142E-1 0.3849	1.1596E-1 0.4873	8.2721E-2 0.5854	5.5130E-2 0.6248	3.5753E-2
2^{-16}	1.5137E-1 0.3861	1.1583E-1 0.4865	8.2678E-2 0.5859	5.5082E-2 0.6238	3.5746E-2
2^{-18}	1.5114E-1 0.3905	1.1530E-1 0.4843	8.2423E-2 0.5882	5.4825E-2 0.6216	3.5633E-2
2^{-20}	1.5014E-1 0.4046	1.1342E-1 0.4857	8.1002E-2 0.5876	5.3902E-2 0.6281	3.4877E-2
$d_2^{N,M}$ p_2^{ini}	1.5142E-1 0.3849	1.1596E-1 0.4873	8.2721E-2 0.5854	5.5130E-2 0.6248	3.5753E-2

$$x_i = \begin{cases} iH, & i = 0, \dots, N/4, \\ x_{N/4} + (i - N/4)h_1, & i = N/4 + 1, \dots, N/2, \\ x_{N/2} + (i - N/2)h_2, & i = N/2 + 1, \dots, 3N/4, \\ x_{3N/4} + (i - 3N/4)h_3, & i = 3N/4 + 1, \dots, N/, \end{cases} \tag{48}$$

where $H = 4(1 - \sigma_3)/N,\ h_1 = 4(\sigma_3 - \sigma_2)/N,\ h_2 = 4(\sigma_2 - \sigma_1)/N,\ h_3 = 4\sigma_1/N$, and the transition parameters $\sigma_1, \sigma_2, \sigma_3$ are defined by

$$\begin{aligned} &\sigma_3 = \min\left\{3/4, \sigma_0\varepsilon_3 \ln N\right\},\ \sigma_2 = \min\left\{2\sigma_3/3, \sigma_0\varepsilon_2 \ln N\right\}, \\ &\sigma_1 = \min\left\{\sigma_2/2, \sigma_0\varepsilon_1 \ln N\right\}. \end{aligned} \tag{49}$$

On this mesh, we use again the simple upwind scheme to discretize in space; to integrate in time, we use also the idea of multi-splitting, combining the fractional implicit Euler method which has six implicit stages with a splitting of the space differential operator in directions and components; in this way, tridiagonal systems must be solved to advance in time.

Fig. 3 displays the numerical approximation for the three components, showing the overlapping boundary layers at $x = 1$ and $y = 1$. In this case, the exact solution of (47) is unknown too and we use the same double mesh principle to approximate the maximum global errors. Tables 5, 6 and 7 show such maximum errors and their corresponding orders of convergence for some values of diffusion parameter ε_3, when ε_2 covers the range $R_2 = \{\varepsilon_2; \varepsilon_2 = \varepsilon_3, 2^{-2}\varepsilon_3, \dots, 2^{-18}\}$ and ε_1 covers the range $R_1 = \{\varepsilon_1; \varepsilon_1 = \varepsilon_2, 2^{-2}\varepsilon_2, \dots, 2^{-22}\}$ and for different values of the discretization parameters N and M, for first, second and third component, respectively. From them, we again observe the almost first order of uniform convergence as it was expected. With this example, it is easy to realize that our technique can be applied to systems which have an arbitrary number of components.

In addition to the robustness of our algorithm, due to the uniform convergence of it, its main advantage is focused on its computational efficiency associated to the special time integrator which we have designed. This technique decouples the components and the spatial directions of the system, in such way that only tridiagonal linear systems must be solved to advance in time. This advantage is clearly showed in [10] for linear one dimensional parabolic systems and in [9,12] for semilinear one dimensional parabolic systems, in comparison with classical implicit methods as the Euler method. In the two dimensional model problems considered in this work, our technique is considerably more efficient because the use of classical implicit methods to discretize in time leads to solve block banded linear systems, via iterative methods. Moreover, as in the case of one dimensional problems, the efficiency of our proposal becomes more remarkable when the number of components in the coupled system increases, because, in these cases, classical implicit methods require to solve more complicated linear systems.

6. Conclusions

In this work, we have dealt with the efficient numerical solution of two dimensional parabolic singularly perturbed systems of convection–diffusion type, when the diffusion parameters at each equation are distinct and they can have different order of magnitude. For this type of problems, in general, for sufficiently small values of the diffusion parameters, overlapping regular boundary layers use to appear at the outflow boundary of the spatial domain. The numerical method that we have constructed combines the classical upwind finite difference scheme, defined on a mesh of Shishkin type, to discretize in space, and the fractional implicit Euler method

Table 5
Estimated maximum and uniform errors and orders of convergence for the component u_1 in problem (47).

ε_3	N = 16 M = 8	N = 32 M = 16	N = 64 M = 32	N = 128 M = 64	N = 256 M = 128
2^{-6}	1.0554E-1 0.5269	7.3250E-2 0.4616	5.3194E-2 0.6276	3.4430E-2 0.6747	2.1570E-2
2^{-8}	1.0769E-1 0.5379	7.4179E-2 0.4494	5.4323E-2 0.6307	3.5086E-2 0.6924	2.1712E-2
2^{-10}	1.0833E-1 0.5407	7.4466E-2 0.4464	5.4650E-2 0.6313	3.5282E-2 0.6955	2.1786E-2
2^{-12}	1.0849E-1 0.5413	7.4546E-2 0.4455	5.4740E-2 0.6314	3.5337E-2 0.6957	2.1818E-2
2^{-14}	1.0852E-1 0.5413	7.4568E-2 0.4453	5.4764E-2 0.6314	3.5352E-2 0.6958	2.1826E-2
$d_1^{N,M}$ p_1^{uni}	1.0852E-1 0.5413	7.4568E-2 0.4453	5.4764E-2 0.6314	3.5352E-2 0.6958	2.1826E-2

Table 6
Estimated maximum and uniform errors and orders of convergence for the component u_2 in problem (47).

ε_3	N = 16 M = 8	N = 32 M = 16	N = 64 M = 32	N = 128 M = 64	N = 256 M = 128
2^{-6}	3.1242E-2 0.1917	2.7356E-2 0.4516	2.0003E-2 0.6792	1.2492E-2 0.8205	7.0736E-3
2^{-8}	3.1522E-2 0.2094	2.7264E-2 0.4499	1.9960E-2 0.6774	1.2481E-2 0.8197	7.0709E-3
2^{-10}	3.1586E-2 0.2136	2.7239E-2 0.4496	1.9945E-2 0.6770	1.2475E-2 0.8194	7.0695E-3
2^{-12}	3.1590E-2 0.2137	2.7241E-2 0.4499	1.9943E-2 0.6768	1.2475E-2 0.8193	7.0700E-3
2^{-14}	3.1390E-2 0.2121	2.7098E-2 0.4483	1.9860E-2 0.6752	1.2437E-2 0.8179	7.0553E-3
$d_2^{N,M}$ p_2^{uni}	3.1590E-2 0.2077	2.7356E-2 0.4516	2.0003E-2 0.6792	1.2492E-2 0.8205	7.0736E-3

Table 7
Estimated maximum and uniform errors and orders of convergence for the component u_3 in problem (47).

ε_3	N = 16 M = 8	N = 32 M = 16	N = 64 M = 32	N = 128 M = 64	N = 256 M = 128
2^{-6}	7.5266E-2 0.4002	5.7034E-2 0.5138	3.9945E-2 0.6147	2.6087E-2 0.7232	1.5802E-2
2^{-8}	7.8389E-2 0.3555	6.1268E-2 0.4296	4.5489E-2 0.5189	3.1746E-2 0.5835	2.1186E-2
2^{-10}	7.9144E-2 0.3404	6.2509E-2 0.4109	4.7018E-2 0.4855	3.3582E-2 0.5208	2.3405E-2
2^{-12}	7.9332E-2 0.3367	6.2820E-2 0.4061	4.7409E-2 0.4765	3.4074E-2 0.5007	2.4082E-2
2^{-14}	7.9379E-2 0.3357	6.2898E-2 0.4049	4.7508E-2 0.4735	3.4216E-2 0.4961	2.4260E-2
$d_3^{N,M}$ p_3^{uni}	7.9379E-2 0.3357	6.2898E-2 0.4049	4.7508E-2 0.4735	3.4216E-2 0.4961	2.4260E-2

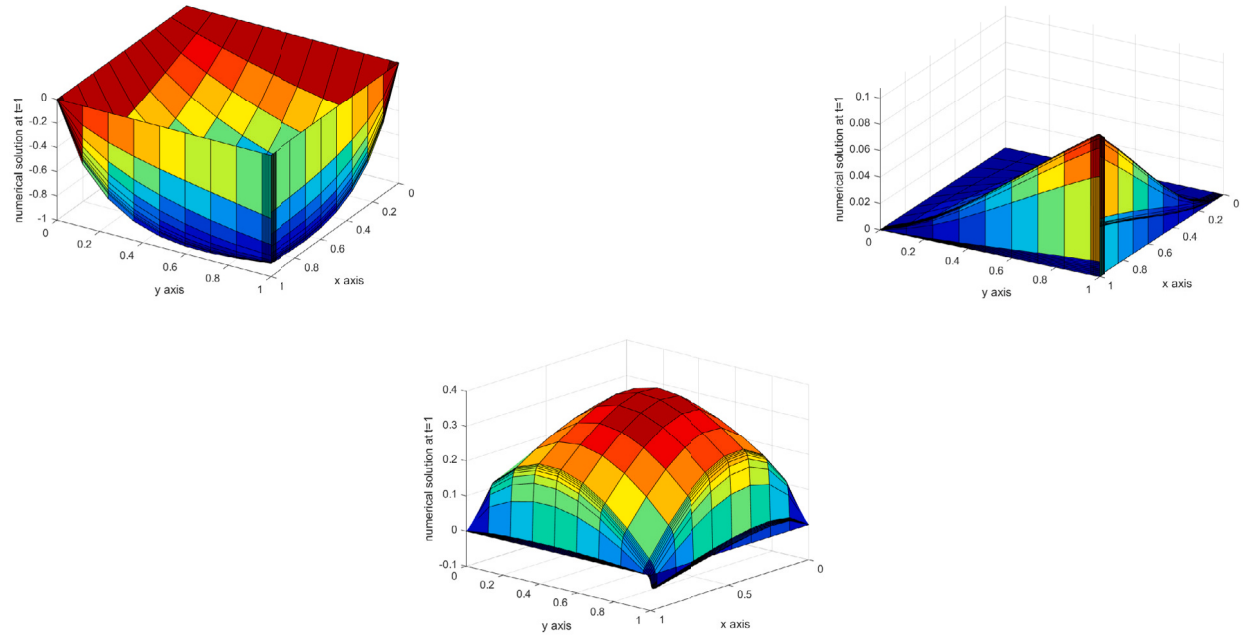

Fig. 3. Components of problem (47) for $\varepsilon_1 = 10^{-6}$, $\varepsilon_2 = 10^{-4}$, $\varepsilon_3 = 10^{-2}$, with $N = M = 32$ (left up u_1, right up u_2, bottom u_3).

together with a splitting by directions and components to discretize in time. Then, the numerical algorithm is uniformly convergent with respect to both diffusion parameters, having first order in time and almost first order in space. The most important quality of the constructed method is that it permits to calculate the numerical solution by solving only tridiagonal linear systems; this feature provides an important reduction in the computational cost of the method with respect to classical methods used for the same type of problems. We have shown the numerical results obtained for different test problems, which corroborate in practice the uniform convergence of the method. As well, we explain and check that the algorithm can be easily extended to coupled systems with a larger number of equations with different diffusion parameters at each equation of the system; from the numerical results obtained for this last example, we see that the efficiency of the algorithm increases with the number of equations in the coupled system.

CRediT authorship contribution statement

C. Clavero: Writing – review & editing, Writing – original draft, Validation, Supervision, Software, Methodology, Investigation, Formal analysis, Conceptualization. **J.C. Jorge:** Writing – review & editing, Writing – original draft, Validation, Supervision, Methodology, Investigation, Conceptualization.

Acknowledgements

The authors thank to the referees for their valuable suggestions which have helped to improve the presentation of this paper. This research was partially supported by the projects PID2022-136441NB-I00 and TED2021-130884B-I00, the Aragón Government and European Social Fund (group E24-17R) and the Public University of Navarra.

References

[1] I. Alonso-Mallo, B. Cano, J.C. Jorge, Spectral-fractional step Runge-Kutta discretizations for initial boundary value problems with time dependent boundary conditions, Math. Compet. 73 (2004) 1801–1825.
[2] G.I. Barenblatt, I.P. Zheltov, L.N. Kochin, Basic concepts in the theory of seepage of homogeneous liquids in fissured rocks, J. Appl. Math. Mech. 24 (1960) 1286–1303.
[3] Z. Cen, Parameter-uniform finite difference scheme for a system of coupled singularly perturbed convection-diffusion equations, Int. J. Comput. Math. 82 (2) (2005) 177–192.
[4] C. Clavero, J. Jorge, F. Lisbona, G. Shishkin, A fractional step method on a special mesh for the resolution of multidimensional evolutionary convection-diffusion problems, Appl. Numer. Math. 27 (3) (1998) 211–231.
[5] C. Clavero, J.C. Jorge, F. Lisbona, G.I. Shishkin, An alternating direction scheme on a nonuiform mesh for reaction-diffusion parabolic problems, IMA J. Numer. Anal. 20 (2) (2000) 263–280.
[6] C. Clavero, J.C. Jorge, Uniform convergence and order reduction of the fractional implicit Euler method to solve singularly perturbed 2D reaction-diffusion problems, Appl. Math. Comput. 287 (88) (2016) 12–27.
[7] C. Clavero, J.C. Jorge, Solving efficiently one dimensional parabolic singularly perturbed reaction-diffusion systems: a splitting by components, J. Comput. Appl. Math. 344 (2018) 1–14.
[8] C. Clavero, J.C. Jorge, An efficient numerical method for singularly perturbed time dependent parabolic 2D convection-diffusion systems, J. Comput. Appl. Math. 354 (2019) 431–444.

[9] C. Clavero, J.C. Jorge, An efficient and uniformly convergent scheme for one dimensional parabolic singularly perturbed semilinear systems of reaction-diffusion type, Numer. Algorithms 85 (2020) 1005–1027.
[10] C. Clavero, J.C. Jorge, A splitting uniformly convergent method for one-dimensional parabolic singularly perturbed convection-diffusion systems, Appl. Numer. Math. 183 (2023) 317–332.
[11] C. Clavero, J.C. Jorge, A multi-splitting method to solve 2D parabolic reaction-diffusion singularly perturbed systems, J. Comput. Appl. Math. 417 (2023), https://doi.org/10.1016/j.cam.2022.114569.
[12] C. Clavero, J.C. Jorge, Efficient numerical methods for one dimensional semilinear parabolic singularly perturbed convection-diffusion systems, Appl. Numer. Math. 198 (2024) 461–473.
[13] C. Clavero, R. Shiromani, V. Shanthi, A numerical approach for a two-parameter singularly perturbed weakly-coupled system of 2-D elliptic convection-reaction-diffusion PDEs, J. Comput. Appl. Math. (2023), https://doi.org/10.1016/j.cam.2023.115422.
[14] C. Clavero, R. Shiromani, V. Shanthi, A computational approach for 2D elliptic singularly perturbed weakly-coupled systems of convection-diffusion type with multiple scales and parameters in the diffusion and the convection terms, Math. Methods Appl. Sci. (2024) 1–32, https://doi.org/10.1002/mma.10204.
[15] A. Das, S. Natesan, Higher-order convergence with fractional-step method for singularly perturbed 2D parabolic convection-diffusion problems on Shishkin mesh, Comput. Math. Appl. 75 (2018) 2387–2403.
[16] A. Das, S. Natesan, Stability and error analysis of a fully-discrete numerical method for system of 2D singularly perturbed parabolic PDEs, Comput. Math. Appl. 110 (2022) 135–145.
[17] I.R. Epstein, I. Lengyel, S. Kádár, M. Kagan, M. Yokoyama, New systems for pattern formation studies, Phys. A, Stat. Mech. Appl. 188 (1992) 26–33.
[18] P.A. Farrell, A.F. Hegarty, J.J.H. Miller, E. O'Riordan, G.I. Shishkin, Robust Computational Techniques for Boundary Layers, Applied Mathematics, vol. 16, Chapman and Hall/CRC, 2000.
[19] L. Govindarao, A. Das, A second-order fractional step method for two-dimensional delay parabolic partial differential equations with a small parameter, Palest. J. Math. 11 (3) (2022) 96–111.
[20] S.S. Kalaiselvan, J.J.H. Miller, S. Valarmathi, A parameter uniform fitted mesh method for a weakly coupled system of two singularly perturbed convection-diffusion equations, Math. Commun. 24 (2) (2019) 193–210.
[21] Y. Kan-On, M. Mimura, Singular perturbation approach to a 3-component reaction-diffusion system arising in population dynamics, SIAM J. Math. Anal. 29 (1998) 1519–1536.
[22] R.B. Kellogg, T. Linss, M. Stynes, A finite difference method on layer-adapted meshes for an elliptic reaction-diffusion system in two dimensions, Math. Comput. 774 (2008) 2085–2096.
[23] R.B. Kellogg, N. Madden, M. Stynes, A parameter robust numerical method for a system of reaction-diffusion equations in two dimensions, Numer. Methods Partial Differ. Equ. 24 (2007) 312–334.
[24] M. Kumar, S. Natesan, Numerical analysis of singularly perurbed system of parabolic convection-diffsuion problem with regular boundary layers, Differ. Equ. Dyn. Syst. (2019), https://doi.org/10.1007/s12591-019-00462-2.
[25] M. Kumar, S. Natesan, A robust computational method for singularly perturbed system of 2D parabolic convection-diffusion problems, Int. J. Math. Model. Numer. Optim. 9 (2019) 127–157.
[26] M. Kumar, S. Natesan, A parameter-uniform hybrid finite difference scheme for singularly perturbed system of parabolic convection-diffusion problems, Int. J. Comput. Math. 97 (4) (2020) 875–905.
[27] O.A. Ladyzhenskaya, V.A. Solonnikov, N.N. Uraltseva, Linear and Quasilinear Equations of Parabolic Type, Translations of Mathematical Monographs, vol. 23, American Mathematical Society, Providence, R.I., 1967.
[28] T. Linss, The necessity of Shishkin decompositions, Appl. Math. Lett. 14 (7) (2001) 891–896.
[29] T. Linss, M. Stynes, Asymptotic analysis and Shishkin-type decomposition for an elliptic convection– diffusion problem, J. Math. Anal. Appl. 261 (2) (2001) 604–632.
[30] T. Linss, M. Stynes, Numerical solution of systems of singularly perturbed differential equations, Comput. Methods Appl. Math. 9 (2009) 165–191.
[31] L.B. Liu, Y. Chen, A robust adaptive grid method for a system of two singularly perturbed convection-diffusion equations with weak coupling, J. Sci. Comput. 61 (2014) 1–16.
[32] L.B. Liu, G. Long, Y. Zhang, Parameter uniform numerical method for a system of two coupled singularly perturbed parabolic convection-diffusion equations, Adv. Differ. Equ. (2018) 450, https://doi.org/10.1186/s13662--018--1907--1, 2018.
[33] G.I. Marchuk, Splitting and alternating direction methods, in: Handbook of Numerical Analysis v. 1, North-Holland Elsevier, 1990, pp. 197–462.
[34] S. Nagarajan, A paramater robust fitted mesh finite difference method for a system ot two reaction-convection-diffusion equations, Appl. Numer. Math. 179 (2022) 87–104.
[35] C.V. Pao, Nonlinear Parabolic and Elliptic Equations, Plenum Press, New York, 1992.
[36] R.M. Priyadharshini, N. Ramanujam, A. Tamilsevan, Hybrid difference schemes for a system of singularly perturbed convection-diffusion equations, J. Appl. Math. Inform. 27 (2009) 1001–1015.
[37] G.P. Thomas, Towards an improved turbulence model for wave-current interactions, in: 2nd Annual Report to EU MAST-III Project The Kinematics and Dynamics of Wave-Current Interactions, 1998.